Reactions of [RhCl(diene)]$_2$ with Bi- and Terdentate Nitrogen Ligands. X-ray Structures of Five-Coordinate Complexes

Hendrikus F. Haarman,† Frank R. Bregman,† Jan-Meine Ernsting,†
Nora Veldman,‡ Anthony L. Spek,‡ and Kees Vrieze*,†

J. H. van't Hoff Research Institute, Laboratorium voor Anorganische Chemie, Universiteit van Amsterdam, Nieuwe Achtergracht 166, 1018 WV Amsterdam, The Netherlands, and Bijvoet Center for Biomolecular Research, Vakgroep Kristal- en Structuurchemie, Universiteit Utrecht, Padualaan 8, 3584 CH Utrecht, The Netherlands

Received September 3, 1996[⊗]

Reaction of [RhCl(diene)]$_2$ (diene = 1,5-cyclooctadiene (COD) or bicyclo[2.2.1] hepta-2,5-diene (NBD)) with the *N*−*N*−*N* nitrogen ligands 2,6-(C(R^1)═N−R^2)$_2$C$_5$H$_3$N in CD_2Cl_2 or CH_2Cl_2 yielded the five-coordinate complexes [RhCl(2,6-(C(H)═N−R^2)$_2$C$_5$H$_3$N)(diene)] (diene = NBD; R^2 = *i*-Pr, *t*-Bu, and *p*-anisyl), which has been isolated for NBD but not for COD. A single-crystal X-ray determination showed that [RhCl(2,6-(C(H)═N−*p*-anisyl)$_2$C$_5$H$_3$N)(NBD)] has a distorted trigonal bipyramidal configuration with the pyridyl N-atom, one imine N-atom, and one alkene double bond in the equatorial plane, while the second alkene bond and the chloride atom occupy the axial positions. This conformation containing one noncoordinated imine moiety is clearly retained at 183 K in CD_2Cl_2, as is also the case for the other complexes. For the COD complexes, the reaction is more complicated, as the intermediates that are observed depend on the substituents R^1 and R^2 of the N−N−N nitrogen ligand. The five-coordinate complexes [RhCl(2,6-(C(R^1)═N−R^2)$_2$C$_5$H$_3$N)(COD)] could be observed at low temperatures for R^1 = H and R^2 = *i*-Pr, *t*-Bu, and *p*-anisyl, while for R^1 = Me and R^2 = *p*-anisyl, this intermediate could not be observed; instead, [Rh(2,6-(C(Me)═N−*p*-anisyl)$_2$C$_5$H$_3$N)$_2$]$^+$Cl$^-$ was found, which shows the presence of one N−N−N ligand bonded as a bidentate ligand and one N−N−N ligand bonded as a terdentate ligand at low temperatures. Further reaction of [Rh(2,6-(C(Me)═N−*p*-anisyl)$_2$C$_5$H$_3$N)$_2$]$^+$Cl$^-$ with [RhCl(COD)]$_2$ afforded [RhCl(2,6-(C(Me)═N−*p*-anisyl)$_2$C$_5$H$_3$N)] and subsequently, via oxidative addition of CD_2Cl_2, the complex [RhCl$_2$(CD_2Cl)(2,6-(C(Me)═N−*p*-anisyl)$_2$C$_5$H$_3$N)]. The dynamic properties of the five-coordinate diene complexes [RhCl(2-(C(H)═N−R^2)-6-(Me)-C$_5$H$_3$N)(NBD)] (R^2 = *i*-Pr, *t*-Bu, and *p*-anisyl), which contain N−N nitrogen ligands, and of the new complexes [Rh(2-(C(H)═N−R^2)-6-(Me)C$_5$H$_3$N)(NBD)]OTf (R^2 = *i*-Pr, *t*-Bu, and *p*-anisyl) and of [Rh(2,2′-bipyrimidine)(NBD)]OTf have been investigated. A single-crystal X-ray determination of [RhCl(2-(C(H)═N−*i*-Pr)-6-(Me)C$_5$H$_3$N)(NBD)] showed structural features which are analogous to those of [RhCl(2,6-(C(H)═N−*p*-anisyl)$_2$C$_5$H$_3$N)(NBD)].

Introduction

Recently we reported novel Rh(I) complexes which were able to cleave C−Cl bonds of reagents such as dichloromethane, chloroform, benzyl chloride, and α,α-dichlorotoluene by oxidative addition.[1] By employment of N−N−N nitrogen ligands of the type 2,6-(C(R^1)═N−R^2)$_2$C$_5$H$_3$N (R^1 = H, R^2 = *i*-Pr, *t*-Bu, cyclohexyl, and *p*-anisyl; R^1 = Me, R^2 = *p*-anisyl and *i*-Pr), we succeeded in preparing very nucleophilic and very reactive Rh(I) complexes via reaction of [RhCl(alkene)$_2$]$_2$ (alkene = cyclooctene or ethene) with the above N−N−N ligands. The molecular structures of [RhCl(2,6-(C(R^1)═N−R^2)$_2$C$_5$H$_3$N)] (R^1 = H, R^2 = *i*-Pr, *t*-Bu; R^1 = Me, R^2 = *i*-Pr) were determined by X-ray analysis. Interestingly, by increasing the steric bulk of R^1 and R^2, the equatorial chloride atom was bent increasingly out of the plane of the molecule, while the nitrogen ligand remained bonded in a terdentate fashion. This distortion of the Cl-atom out of the coordination plane could be correlated with very large shifts of the ^{103}Rh resonances to high parts per million values owing to changes in the molecular orbital sequence.[2] In this context, it should be noted that while we were unable to incorporate ethene or cyclooctene in the product, alkene-containing rhodium complexes with phosphine ligands have been reported, *e.g.*, by Burgess *et al.*[3] and Binger *et al.*[4] The Rh(III) complexes [RhCl$_2$(R^3)(2,6-(C(R^1)═N−R^2)$_2$C$_5$H$_3$N)] (R^3 = CH_2Cl, $CHCl_2$, CH_2Ph, CHClPh, and Cl) resulting from reactions of the Rh(I) complexes with the appropriate substrates show the expected six-coordinate geometry. However, for R^1 = Me and R^2 = *i*-Pr, it was shown by variable temperature ^{1}H NMR experiments that in

* To whom correspondence should be addressed.
† J. H. van't Hoff Research Institute.
‡ Bijvoet Center for Biomolecular Research.
⊗ Abstract published in *Advance ACS Abstracts,* December 1, 1996.
(1) Haarman, H. F.; Ernsting, J. M.; Kranenburg, M.; Kooijman, H.; Veldman, N.; Spek, A. L.; van Leeuwen, P. W. N. M.; Vrieze, K. To be published.
(2) Haarman, H. F.; Kaagman, J. W. F.; Ernsting, J. M.; Wilms, M.; Vrieze, K.; Elsevier, C. J. To be published.
(3) Burgess, K.; van der Donk, W. A.; Westcott, S. A.; Marder, T. B.; Baker, R. T.; Calabrese, J. C. *J. Am. Chem. Soc.* **1992**, *114*, 9350.
(4) Binger, P.; Haas, J.; Glaser, G.; Goddard, R.; Krüger, C. *Chem. Ber.* **1994**, *127*, 1927.

S0276-7333(96)00760-1 CCC: $14.00

solution there is an equilibrium between a six-coordinate Rh(III) species and an unusual five-coordinate Rh(III) form which contains a bidentate bonded N−N−N ligand and is the dominant species at higher temperatures. Molecular modeling of the complexes with R^1 = Me, R^2 = *i*-Pr, and R^3 = CH_2Cl, $CHCl_2$, CH_2Ph, CHClPh, and Cl based on the data of the X-ray structures of [RhCl(2,6-(C(R^1)=N−R^2)$_2$$C_5H_3N$)] ($R^1$ = H, R^2 = *i*-Pr, *t*-Bu; R^1 = Me, R^2 = *i*-Pr) and [$RhCl_2$(CH_2Cl)(2,6-(C(H)=N−R^2)$_2$$C_5H_3N$)] ($R^2$ = *i*-Pr and cyclohexyl) showed steric interactions between the methyl groups of the *i*-Pr group (R^2) and the methyl group (R^1) and between the *i*-Pr (R^2) methyl groups and the chloride atom(s) or the phenyl substituent of the R^3 group. For R^1 = Me and R^2 = *i*-Pr this led to the formation of the five-coordinate Rh(III) complexes.

In order to shed more light on the intimate pathways by which the complexes [RhCl(2,6-(C(R^1)=N−R^2)$_2$$C_5H_3N$)] are formed from Rh(I)−alkene complexes, we directed our attention to substitution reactions of [RhCl(diene)]$_2$ (diene = 1,5-cyclooctadiene (COD) or bicyclo[2.2.1]hepta-2,5-diene (NBD)) with the N−N−N nitrogen ligands 2,6-(C(R^1)=N−R^2)$_2$$C_5H_3N$ (R^1 = H, R^2 = *i*-Pr, *t*-Bu, and *p*-anisyl; R^1 = Me, R^2 = *i*-Pr and *p*-anisyl). To facilitate the characterization of the intermediate species, we have studied the reaction of the N−N nitrogen ligands 2-(C(H)=N−R^2)-6-(Me)C_5H_3N (R^2 = *i*-Pr, *t*-Bu, and *p*-anisyl) and 2,2′-bipyrimidine with [RhX(NBD)]$_2$ (X = Cl, OTf). The results show that the substitution reactions, the intermediates, and the dynamic behavior of the intermediates critically depend on both the alkene and the substituents R^1 and R^2 of the N−N−N ligand.

Experimental Section

All experiments were carried out in a dry nitrogen atmosphere using standard Schlenk techniques. Benzene, diethyl ether, tetrahydrofuran (THF), and pentane were distilled before use from sodium/benzophenone, dichloromethane and chloroform were distilled from calcium hydride, and acetone was distilled from $KMnO_4$/Na_2CO_3. Molecular sieves, 3 Å, were activated at 180 °C *in vacuo* for 24 h. Deuterobenzene was dried over sodium and stored under nitrogen. Deuterated chlorinated solvents were dried with molecular sieves, 3 Å, and stored under nitrogen. The ^{1}H and ^{13}C NMR spectra were recorded on a Bruker AMX 300 or AC 200 spectrometer. The spectra were indirectly referenced to TMS using residual solvent signals. Fast atom bombardment mass spectrometry (FABMS) was carried out by the Institute for Mass Spectroscopy of the University of Amsterdam using a JEOL JMS SX/SX102A four-sector mass spectrometer coupled to a JEOL MS-7000 data system. The samples were loaded in a matrix solution (nitrobenzyl alcohol) onto a stainless steel probe and bombarded with xenon atoms with an energy of 3 keV. During the high-resolution FABMS measurements, a resolving power of 5000 (10% valley definition) was used. CsI and/or glycerol was used to calibrate the mass spectrometer. Elemental analyses were carried out by Dornis und Kolbe, Mikroanalytisches Laboratorium, Mülheim a.d. Ruhr, Germany, and by our Institute. The conductometric experiments were carried out with a Consort K 720 conductometer equipped with a Philips PW 9512/00 conductometric cell in a closed glass vessel.

2,2′-Bipyrimidine (bpm, **1**) and AgOTf (OTf = trifluoromethanesulfonate) were obtained from Aldrich and used as received. The N−N nitrogen ligands[5] 2-(C(H)=N−R^2)-6-(Me)-C_5H_3N (R^2 = *i*-Pr (**2**), *t*-Bu (**3**), and *p*-anisyl(**4**)), the N−N−N nitrogen ligands[5] 2,6-(C(R^1)=N−R^2)$_2$$C_5H_3N$ (R^1 = H, R^2 = *i*-Pr (**5**), *t*-Bu (**6**), and *p*-anisyl (**7**); R^1 = Me, R^2 = *i*-Pr (**8**) and *p*-anisyl (**9**)), [RhCl(COD)]$_2$[6] (COD = 1,5-cyclooctadiene), and [RhCl(NBD)]$_2$[6] (NBD = norbornadiene = bicyclo[2.2.1]hepta-2,5-diene) were synthesized according to literature procedures. The ligands were purified by either sublimation or crystallization, depending on the ligand.

[Rh(bpm)(NBD)]OTf (10). To a solution of 0.0660 g of [RhCl(NBD)]$_2$ (1.4×10^{-4} mol) in 5 mL of dichloromethane was added 0.0737 g of AgOTf (2.9×10^{-4} mol). The resulting suspension was stirred for 1 h and subsequently filtered giving a clear yellow solution. A solution of 0.366 g of bpm (**1**, 2.8×10^{-4} mol) in 5 mL of dichloromethane was added giving a red-brown precipitate, which was filtered off, washed with dichloromethane (4 × 5 mL), and dried *in vacuo*. Yield: 0.10 g of **10** (85%). The complex is black-brown and dissolves only very slightly, even in polar solvents. The analysis is slightly off owing to solvent incorporation. However, the FABMS measurement is conclusive.

Anal. Calcd for $C_{16}H_{14}F_3N_4O_3RhS$ (**10**): C, 38.26; H, 2.81; N, 11.15. Found: C, 37.77; H, 3.22; N, 10.53. FABMS for **10** ($C_{16}H_{14}F_3N_4O_3RhS$) (obsd *m/z*, *calcd m/z*): 501.9738, *501.9786*.

^{1}H NMR of Mixtures of Free Ligand 1 and Complex 10 as a Function of Temperature. ^{1}H NMR spectra were recorded at 183 and 293 K of a saturated solution of **10** in 0.5 mL of CD_2Cl_2. Subsequently, variable temperature ^{1}H NMR spectra were measured on the same solution to which 2 equiv of free bpm ligand (**1**) had been added. As the signals of the coordinated and noncoordinated bpm had coalesced, intermolecular exchange of bpm appeared to occur. It was unfortunately not possible to study the kinetics of the reaction, owing to insolubility of **10**.

Synthesis of [Rh(2-(C(H)=N−R^2)-6-(Me)C_5H_3N)(NBD)]-OTf (R^2 = *i*-Pr (11), *t*-Bu (12), and *p*-Anisyl (13)). A representative synthesis is given for complex **11**. [RhCl-(NBD)]$_2$ (0.0946 g, 2.05×10^{-4} mol) was added to 0.11 g of AgOTf (4.3×10^{-4} mol) in 20 mL of dichloromethane. The resulting suspension was stirred for 1 h and subsequently filtered giving a clear yellow-orange solution to which 80 μL of the N−N ligand **2** (0.073 g, 4.5×10^{-4} mol) was added. Dichloromethane was evaporated *in vacuo* giving a sticky residue, and after the residue was washed with diethyl ether (3 × 5 mL) and cold THF (2 × 1 mL) and dried *in vacuo*, the product was isolated as a red powder. Yield: 0.174 g (84%). The yield of **12** was 70% and that of **13** was 85%. Anal. Calcd for $C_{18}H_{22}F_3N_2O_3RhS$ (**11**): C, 42.70; H, 4.38; N, 5.53. Found: C, 42.61; H, 4.82; N, 4.59. Anal. Calcd for $C_{19}H_{24}F_3N_2O_3RhS$ (**12**): C, 43.94; H, 4.47; N, 5.39. Found: C, 44.07; H, 4.78; N, 5.38. FABMS for **11** ($C_{18}H_{22}F_3N_2O_3RhS$) (obsd *m/z*, *calcd m/z*): 506.0393, *506.0358*. FABMS for **12** ($C_{19}H_{24}F_3N_2O_3RhS$) (obsd *m/z*, *calcd m/z*): 520.0595, *520.0515*. FABMS for **13** ($C_{22}H_{22}F_3N_2O_4RhS - CF_3SO_3$) (obsd *m/z*, *calcd m/z*): 421.0746, *421.0780*.

^{1}H NMR of Mixtures of Free Ligand 2 and Complex 11 as a Function of Temperature. A NMR tube was filled with 0.0061 g of **11** (1.2×10^{-5} mol, 0.022 mol/L) and 0.72 g of CD_2Cl_2 (0.55 mL). ^{1}H NMR spectra were recorded at 183 and 263 K. Subsequently, variable temperature ^{1}H NMR spectra were recorded on the same solutions to which 1.0 μL of the free N−N ligand **2** (0.93×10^{-3} g, 0.58×10^{-5} mol) had been added. Similar measurements were carried out after adding excess free N−N ligand **2** as follows: 1.2 μL (0.71×10^{-5} mol, 1.0 equiv), 1.5 μL (0.84×10^{-5} mol, 1.8 equiv), and 1.7 μL (1.0×10^{-5} mol, 2.5 equiv). It was found that intermolecular exchange of the free ligand took place. The reciprocal lifetime ($1/\tau$) values at 263 K were calculated by using the line widths of the Me (H5, Scheme 1) signal of complex **11** as a function of the free ligand concentration at 263 K. (c [mol/L], $1/\tau$ [s^{-1}]): c = 0.011, $1/\tau$ = 8.8; c = 0.023, $1/\tau$ = 19.5; c = 0.039, $1/\tau$ = 34.9; c = 0.057, $1/\tau$ = 51.5. These $1/\tau$ values were also calculated by using the line widths of the Me (H5) signal of

(5) Lavery, A.; Nelson, S. M. *J. Chem. Soc., Dalton Trans.* **1985**, 1053.

(6) van der Ent, A.; Onderdelinden, A. L. *Inorg. Synth.* **1990**, *28*, 90.

the free ligand (0.010 mol/L) as a function of the concentration of complex **11** at 263 K. (c [mol/L], $1/\tau$ [s^{-1}]): $c = 0.003$, $1/\tau = 1.3$; $c = 0.006$, $1/\tau = 3.8$; $c = 0.012$, $1/\tau = 7.8$; $c = 0.015$, $1/\tau = 9.7$.

Synthesis of [RhCl(2-(C(H)═N−R²)-6-(Me)C₅H₃N)(NBD)] (R² = *i*-Pr (14), *t*-Bu (15), and *p*-Anisyl (16)). A representative synthesis is presented for complex **16**. To a solution of 0.025 g of $[RhCl(NBD)]_2$ (5.0×10^{-5} mol) in 1 mL of dichloromethane was added a solution of 0.021 g of **4** (10×10^{-5} mol) in 1 mL of dichloromethane at 195 K. After the red solution was warmed to room temperature, dichloromethane was evaporated giving a sticky residue, which was washed with benzene (3 × 1 mL) and pentane (3 × 1 mL). The resulting red powder, was dried *in vacuo*. Yield: 0.036 g (7.8×10^{-5} mol, 78%). The yield of **14** is 75% and that of **15** is 85%.

Anal. Calcd for $C_{17}H_{22}ClN_2Rh$ (**14**): C, 51.98; H, 5.65; N, 7.13. Found: C, 51.84; H, 5.66; N, 7.17. Anal. Calcd for $C_{18}H_{24}ClN_2Rh$ (**15**): C, 53.15; H, 5.95; N, 6.89. Found: C, 53.20; H, 6.04; N, 6.94. Elemental analysis of **16** was not carried out, as **16** is completely analogous to **14** and **15**. FABMS for **14** ($C_{17}H_{22}ClN_2Rh$) (obsd *m/z*, *calcd m/z*): 392.0500, *392.0519*. FABMS for **15** ($C_{18}H_{24}ClN_2Rh$) (obsd *m/z*, *calcd m/z*): 406.0690, *406.0676*. FABMS for **16** ($C_{21}H_{22}ClN_2ORh$) (obsd *m/z*, *calcd m/z*): 456.0450, *456.0468*.

¹H NMR of Mixtures of Free Ligand 2 and Complex 14 as a Function of Temperature. A NMR tube was filled with 0.0055 g of **14** (1.4×10^{-5} mol) which was dissolved in 0.83 g (0.63 mL) of CD_2Cl_2. At 294, 243, and 183 K, ^{1}H NMR spectra were measured. After 1.2 μL (7.0×10^{-6} mol) and 4.8 μL (28×10^{-6} mol) of free ligand **2** were added, ^{1}H NMR spectra were recorded at the same temperatures. Addition of free ligand had no effect on the exchange rate, as the ^{1}H NMR signals of complex **14** and of the free ligand **2** were unaffected, showing the absence of intermolecular exchange of the N−N nitrogen ligand on the NMR time scale.

Intermolecular Exchange of Cl⁻ between 11 and 14 and 12 and 15. A representative measurement is presented for complexes **11** and **14**. A NMR tube was filled with 0.0045 g of **11** (8.8×10^{-6} mol), 0.0035 g of **14** (8.9×10^{-6} mol), and 0.79 g (0.60 mL) of deuterodichloromethane. At 183 and 293 K, ^{1}H NMR spectra were recorded. The signals of complexes **11** and **14** could not be observed separately. At 183 K, the signals had already coalesced at the weighted mean, which indicates very fast exchange of Cl^- between **11** and **14**. Similar measurements for mixtures of **12** and **15** showed an analogous behavior.

Synthesis of [RhCl(2,6-(C(H)═N−R²)₂C₅H₃N)(NBD)] (R² = *i*-Pr (17), *t*-Bu (18), and *p*-Anisyl (19)). A representative synthesis is given for complex **19**. To a solution of 0.22 g of $[RhCl(NBD)]_2$ (0.47 mmol) in 50 mL of dichloromethane was added a solution of 0.32 g of the N−N−N ligand **7** (0.95 mmol) in 5 mL of dichloromethane at 298 K affording a red colored solution. The reaction mixture was concentrated to a small volume, and pentane was added, after which fast crystallization occurred. The product could be recrystallized from a small volume of dichloromethane at −20 °C as block-shaped red crystals. Yield: 0.42 g (0.87 mmol, 93%) of pure product. The yields of the other compounds varied from 90 to 97%.

Anal. Calcd for $C_{28}H_{27}ClN_3O_2Rh$ (**19**): C, 58.39; H, 4.72; N, 7.29. Found: C, 58.04; H, 4.56; N, 7.25. FABMS for **17** ($C_{20}H_{31}ClN_3Rh$) (obsd *m/z* − Cl, *calcd m/z* − *Cl*): 412.1243, *412.1253*. FABMS for **18** ($C_{22}H_{31}ClN_3Rh$) (obsd *m/z*, *calcd m/z*): 475.1248, *475.1254*. FABMS for **19** ($C_{28}H_{27}ClN_3O_2Rh$) (obsd *m/z*, *calcd m/z*): 575.0905, *575.0840*.

¹H NMR of Mixtures of Free Ligand 6 and Complex 18 as a Function of Temperature. A NMR tube was filled with 0.0037 g of **18** (7.7×10^{-6} mol) and 0.710 g of CD_2Cl_2 (0.500 mL). ^{1}H NMR spectra were recorded at 183, 204, and 298 K. After 0.0010 g of the N−N−N ligand **6** (4.1×10^{-6} mol) was added, ^{1}H NMR spectra were recorded at the same temperatures. The addition of free ligand had no effect on the widths and positions of the ^{1}H NMR signals of **18** showing the absence of intermolecular ligand exchange.

Study of the *in Situ* Formation of [RhCl(2,6-(C(H)═N−R²)₂C₅H₃N)(COD)] (R² = *i*-Pr (20), *t*-Bu (21), and *p*-Anisyl (22)). A representative measurement is given for the yellow complex **21**. At 195 K, a NMR tube was filled with 0.0090 g of $[RhCl(COD)]_2$ (1.83×10^{-5} mol) and 0.0089 g of **6** (3.65×10^{-5} mol) in 0.79 mL of deuterodichloromethane. ^{1}H NMR spectra were recorded between 183 and 293 K. At 223 K, complex **21** was formed, while in the range of 233−273 K, the equilibrium shifted toward $[RhCl(COD)]_2$ and free ligand.

The red-orange complex **20** was formed at 230 K, and after 1 day at room temperature, the yellow-orange deuterochloromethyl complex $[RhCl_2(CD_2Cl)(2,6\text{-}(C(H)═N\text{-}i\text{-}Pr)_2C_5H_3N)]$ (**23**)[1] was produced. The purple complex **22** was formed at 230 K and decomposed after 24 h at room temperature. The N−N−N ligand **8** did not react with $[RhCl(COD)]_2$. The intermediates **20**, **21**, and **22** could not be isolated.

Study of the *in Situ* Formation of [Rh(2,6-(C(Me)═N−*p*-anisyl)₂C₅H₃N)₂]Cl (24). A NMR tube was filled at 195 K with 0.0050 g of $[RhCl(COD)]_2$ (1.0×10^{-5} mol) and 0.0081 g of **9** (2.1×10^{-5} mol) in 1.0 mL of deuterodichloromethane. ^{1}H NMR spectra were recorded between 183 and 293 K. In the range of 190−240 K, the dark green complex **24** was formed, which could not be isolated. Increasing the temperature caused **24** to react with excess $[RhCl(COD)]_2$ to form the dark green complex $[RhCl(2,6\text{-}(C(Me)═N\text{-}p\text{-anisyl})_2C_5H_3N)]$ (**25**), which was not isolated from the mixture but identified by comparison with an authentic sample.[1] Oxidative addition of deuterodichloromethane to **25** took place at 298 K yielding quantitatively the orange-yellow $[RhCl_2(CD_2Cl)(2,6\text{-}(C(Me)═N\text{-}p\text{-anisyl})_2C_5H_3N)]$ (**26**).

Conductometry. A representative measurement is presented for complex **15**. At 293 K, 0.0053 g of **15** (1.3×10^{-5} mol, 1.3×10^{-3} mol/L) was dissolved in 10.0 mL of distilled dichloromethane and the conductivity was measured. The molar conductivities of the other complexes were measured for concentrations varying between 1.0 and 2.0 mmol/L in dichloromethane at 293K. The conductivity values Λ (Ω^{-1} cm^2 mol^{-1}) at 293 K are as follows: **11**, 69; **12**, 56; **13**, 52; **14**, 2.2; **15**, 1.3; and **16**, 2.1.

Calculation of $\Delta G^{\ddagger}$.[7] The $\Delta G^{\ddagger}$(coalescence) values are 37 ± 2 kJ/mol for **11** (measured on H(12) at 195 K) and 46 ± 2 kJ/mol for **15** (measured on H(12) at 228 K). The values for **18** are 39 ± 2 kJ/mol (measured on H(4) at 218 K), 41 ± 2 kJ/mol (measured on H(7) at 208 K), and 41 ± 2 kJ/mol (measured on H(12) at 208 K).

X-ray Structure Determination of 14 and 19. Crystals of **14** (orange) and **19** (red) were glued to the tip of a Lindemann glass capillary (inert oil technique) and transferred into the cold nitrogen stream of an Enraf-Nonius CAD 4 T diffractometer on a rotating anode. Accurate unit-cell parameters were derived from a least-squares fit of the setting angles of 25 reflections (SET$_4$)[8] in the range $11 < \theta < 14°$. The unit cell was checked for higher lattice symmetry.[9] Crystal data and details on collection and refinement are presented in Table 1. An empirical correction for absorption was done with DIFABS[10] for both complexes. The structures were solved by automated Patterson/Fourier techniques (DIRDIF92).[11] The structures of F^2 were refined by full-matrix least-squares techniques (SHELXL93).[12] Hydrogen atoms were taken into account at calculated positions except for those on C(22), C(23), C(25), and C(26) for **14**, that were located from a difference map, and their positional parameters were refined. The

(7) Faller, J. W. *Adv. Organomet. Chem.* **1977**, *16*, 211.
(8) de Boer, J. L.; Duisenberg, A. J. M. *Acta Crystallogr.* **1984**, *A40*, C410.
(9) Spek, A. L. *J. Appl. Crystallogr.* **1988**, *21*, 578.
(10) Walker, N.; Stuart, D. *Acta Crystallogr.* **1983**, *A39*, 158.
(11) Beurskens, P. T.; Admiraal, G.; Beurskens, G.; Bosman, W. P.; Garcia-Granda, S.; Gould, R. O.; Smits, J. M. M.; Smykalla, C. *The DIRDIF program system: Technical report of the crystallographic laboratory.*; Univerisity of Nijmegen: Nijmegen, The Netherlands, 1992.
(12) Sheldrick, G. M. *SHELXL93. Program for Crystal structure refinement.*; University of Göttingen: Germany, 1993.

Table 1. Crystallographic Data for 14 and 19

	14	19
	Crystal Data	
formula	$C_{17}H_{22}ClN_2Rh$	$C_{28}H_{27}ClN_3O_2\cdot 3/2CH_2Cl_2$
molecular weight	392.73	703.30
crystal system	orthorhombic	monoclinic
space group	*Pbca* (no. 61)	$P2_1/c$ (no. 14)
a (Å)	8.5907(8)	10.5446(7)
b (Å)	12.9657(9)	14.6353(7)
c (Å)	29.014(5)	21.2040(7)
β (deg)		115.845(4)
V (Å^3)	3231.7(7)	2945.0(3)
D_{calc} (g cm^{-3})	1.614	1.586
Z	8	4
F(000)	1600	1428
μ (Mo Kα) (cm^{-1})	12.2	9.6
crystal size (mm)	0.10 × 0.38 × 0.63	0.75 × 0.63 × 0.25
	Data Collection	
T (K)	150	175
θ_{min}, θ_{max}	1.4, 27.4	1.8, 27.4
wavelength (Å)	0.710 73 (Mo Kα)	0.710 73 (Mo Kα)
scan type	ω	$\omega/2\Theta$
$\Delta\omega$ (deg)	0.69 + 0.35 tan Θ	0.58 + 0.35 tan Θ
data set	0:11; −13:16; 0:37	−13:13; −18:0; −27:20
total data	6270	9597
total unique data	3686 (R_{int} = 0.062)	6719 (R_{int} = 0.021)
total obsd [$I > 2\sigma(I)$]	2346	5432
DIFABS corr. range	0.69:1.57	0.91:1.11
	Refinement	
no. of refined params	205	345
final R_1[a]	0.052	0.040
final wR_2[b]	0.113	0.103
goodness of fit (*S*)	1.00	1.04
weighting scheme[c] (w^{-1})	$\sigma^2(F_o^2) + (0.0327P)^2$	$\sigma^2(F_o^2) + 0.049P^2 + 3.19P$
min and max residual density (e Å^{-3})	−0.80, 0.62	−0.79, 0.95

[a] $R_1 = \sum(|F_o| - |F_c|)/\sum|F_o|$. [b] $wR_2 = \{\sum w(F_o^2 - F_c^2)^2/\sum w(F_o^2)^2\}^{1/2}$. [c] $P = (\max(F_o^2, 0) + 2F_c^2)/3$.

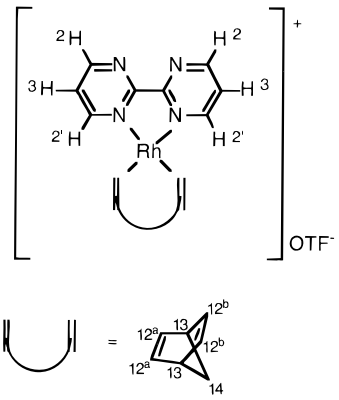

Figure 1. Proposed structure of complex **10**.

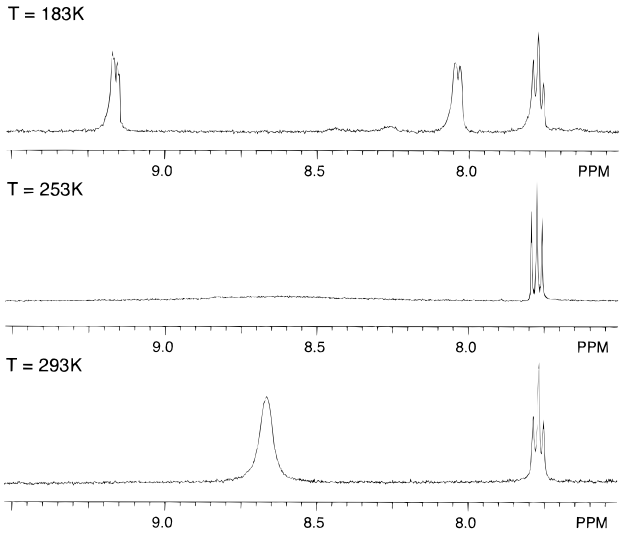

Figure 2. ^{1}H NMR spectra in the region 9.6−7.6 ppm of **10** at 183, 253, and 293 K.

contribution of a disordered $CHCl_3$ on an inversion center for **19** was taken into account following the BYPASS procedure[13] as implemented as the SQUEEZE option in PLATON.[14] Neutral atom scattering factors and anomalous dispersion corrections were taken from the International Tables for Crystallography.[15] Geometrical calculations and illustrations were performed by PLATON.[14]

Results

Synthesis and Characterization of [Rh(bpm)(NBD)]OTf (10). For compound **10** (Figure 1), which was prepared from [RhOTf(NBD)] and bpm (**1**), the ^{1}H NMR spectra (Table 4, Figure 2) at 183 K showed two signals from the bpm ligand belonging to H(2) at 9.16 ppm, with a ^3J(H(2)−H(3)) coupling constant of 5.0 Hz, and to H(2′) at 8.04 ppm, also with a ^3J(H(2′)−H(3)) coupling constant of 5.0 Hz. At 253 K, the signals disappeared in the base line and finally coalesced at 293 K. The temperature had no effect on the position of H(3), since at 183 K, 253 K, and 293 K, H(3) resonates at 7.77 ppm (Figure 2). We have found by measuring the ^{1}H NMR spectra of mixtures of complex **10** and bpm at 183 K that in addition to this intramolecular exchange, intermolecular exchange of the bpm ligand occurs. At this temperature, *e.g.*, for a mixture of 2 equiv of bpm per equiv of complex **10**, the signals of the coordinated and noncoordinated bpm have coalesced.

(13) van der Sluis, P.; Spek, A. L. *Acta Crystallogr.* **1990**, *A46*, 194.
(14) Spek, A. L. *Acta Crystallogr.* **1990**, *A46*, C34.
(15) Wilson, A. J. C. *International Tables for Crystallography*; Kluwer Academic Publishers: Dordrecht, The Netherlands, 1992; Vol. C.

Table 2. ^{1}H NMR[a] Data of the Ligands 2−9

ligand	H(2)	H(3)	H(4)	H(5)	H(6) *H(8)*	H(7)
2[b]	7.81 [d, 1H] 7.15 [d, 1H]	7.60 [d, 1H]	8.37 [s, 1H]	2.58 [s, 3H]	3.62 [sp 1H]	1.26 [d, 6H]
3[c]	7.79 [d, 1H] 7.16 [d, 1H]	7.61 [t, 1H]	8.29 [s, 1H]	2.54 [s, 3H]		1.29 [s, 9H]
4[b]	8.00 [d, 1H] 7.32 [d, 1H]	7.87 [t, 1H]	8.61 [s, 1H]	2.53 [s, 3H]	*3.83 [s, 3H]*	7.33 [d, 2H] 6.94 [d, 2H]
5[b,d]	8.03 [d, 2H]	7.79 [t, 1H]	8.44 [s, 2H]		3.66 [sp, 2H]	1.29 [d, 12H]
6[c,d]	8.01 [d, 2H]	7.79 [t, 1H]	8.36 [s, 2H]			1.31 [s, 18H]
7[c,d]	8.25 [d, 2H]	7.92 [t, 1H]	8.67 [s, 2H]		*3.86 [s, 6H]*	6.97 [d, 4H] 7.36 [d, 4H]
8[b,d]	8.06 [d, 2H]	7.68 [t, 1H]		2.40 [s, 3H]	3.93 [sp, 2H]	1.24 [d, 12H]
9[b,d]	8.27 [d, 2H]	7.89 [t, 1H]		2.37 [s, 3H]	*3.84 [s, 6H]*	6.84 [d, 4H] 6.95 [d, 4H]

[a] ^{1}H NMR spectra were recorded at room temperature at 300.13 MHz; s = singlet, d = doublet, t = triplet, sp = septet. [b] $CDCl_3$. [c] CD_2Cl_2. [d] Taken from ref 1.

Table 3. ^{13}C NMR Data of the Ligands 2−9

ligand	C(1)	C(2)	C(3)	C(4)	C(5)	C(6)	C(7)	C(8)
2[a,b]	158.3, 154.9	124.2, 118.2	136.8	159.8	24.4	61.7	24.3	
3[a,b]	158.0, 155.5	123.9, 117.7	136.7	156.9	24.3	65.9	29.7	
4[a,b]	159.3, 158.8	124.7, 118.7	137.0	159.2	24.5	154.8, 144.3	122.9, 114.8	55.8
5[b,d]	155.1	122.6	137.5	159.6		61.9	24.5	
6[c,d]	156.0	122.0	137.6	156.8		58.5	30.0	
7[c,d]	158.3	123.0	137.7	158.3		144.1,[e] 156.0[f]	115.0, 123.3	56.0
8[b,d]	156.4	120.8	136.3	163.5	13.1	51.3	23.2	
9[b,d]	156.8	122.7	137.3	167.9	16.7	144.3,[e] 156.3[f]	114.8, 121.4	56.0

[a] ^{13}C NMR spectra were recorded at room temperature at 50.32 MHz. [b] CD_2Cl_2. [c] $CDCl_3$. [d] ^{13}C NMR spectra were recorded at room temperature at 75.47 MHz and were taken from ref 1. [e] C(6). [f] Para-C(6′).

Table 4. ^{1}H NMR[a] of the Four-Coordinate Ionic Complexes 10−13

no. (*T* (K))	H(2)	H(3)	H(4)[d]	H(5)	H(6)*H(8)*	H(7)	H(12)	H(13)	H(14)
10[c] (293)	8.67 [br s, 4H]	7.77 [t, 2H]					4.47 [s,[e] 4H]	4.11 [s,[e] 2H]	1.26 [s,[e] 2H]
10[c] (183)	8.16 [dd, 2H] 8.04 [dd, 2H]	7.78 [t, 2H]					4.49 [s,[e] 4H]	4.10 [s,[e] 2H]	1.48 [s,[e] 2H]
11[c] (293)	7.84 [d, 1H] 7.41 [d, 1H]	7.93 [t, 1H]	8.45 (2.6) [d, 1H]	2.26 [s, 3H]	3.14 [sp, 1H]	1.29[g] [d, 6H]	4.45 (2.1)[d] [dd, 4H][g]	4.07 [s,[e] 2H]	1.46 [t, 2H]
11[c] (183)	7.36 [d, 1H] 7.74 [d, 1H]	7.91 [t, 1H]	8.36[f] [s, 1H]	2.16 [s, 3H]	2.99 [sp, 1H]	1.18[g] [br d, 6H]	4.64 [s,[e] 2H][g] 4.08 [s,[e] 2H][g]	4.02 [s,[e] 2H]	1.36 [s,[e] 2H]
12[c] (293)	7.84 [d, 1H] 7.38 [d, 1H]	7.99 [t, 1H]	8.33 (2.4) [d, 1H]	2.28 [s, 3H]		1.29[g] [s, 9H]	4.55 (2.1)[d] [dd, 4H][g]	3.95 [s,[e] 2H]	1.42 [t, 2H]
12[c] (183)	7.57 [d, 1H] 7.33 [d, 1H]	7.95 [t, 1H]	8.20[f] [s, 1H]	2.17 [s, 3H]		1.18[g] [s, 9H]	4.47 [s,[e] 4H][g]	3.89 [s,[e] 2H]	1.32 [s,[e] 2H]
13[b] (293)	7.99 [d, 1H] 7.34 [d, 1H]	7.91 [t, 1H]	8.51 (2.1) [d, 1H]	2.50 [s, 3H]	*3.83 [s, 3H]*	7.32 [d, 2H] 6.92 [d, 2H]	3.95 [dd, 4H]	3.85 [s,[e] 2H]	1.25 [s,[e] 2H]

[a] ^{1}H NMR spectra were recorded at 300.13 MHz; s = singlet, d = doublet, dd = double doublet, t = triplet, sp = septet, br = broad. [b] $CDCl_3$. [c] CD_2Cl_2. [d] J(Rh−H). [e] No coupling observed. [f] Owing to line broadening, no $J(^{103}Rh-H(4))$ could be observed. [g] There is a clear temperature dependent chemical shift varying between 0.08 and 0.36 ppm. [h] J(H−H) in Hz.

Synthesis and Characterization of [Rh(2-(C(H)=N−R^2)-6-(Me)C$_5$H$_3$N)(NBD)]OTf (R^2 = *i*-Pr (11), *t*-Bu (12), and *p*-Anisyl (13)). Complexes **11**−**13** have been synthesized in quantitative yield in dichloromethane by reaction of the corresponding N−N ligands **2**−**4** with [RhOTf(NBD)], which was prepared from $[RhCl(NBD)]_2$ and AgOTf (Scheme 1). Coordination of NBD and the N−N ligands could be inferred from the chemical shift differences between the free and coordinated ligands (Table 2−5). The complexes **11**−**13** could not be stored longer than 1 day, owing to decomposition.

At 183 K, as expected, the nonequivalent olefinic hydrogen atoms H(12[a]) and H(12[b]) of **11** (Scheme 1) have been observed as two signals, since **11** has C_s symmetry, while at 195 K, the signals of H(12[a]) and of H(12[b]) have coalesced. The nonequivalent olefinic hydrogen atoms could only be observed as separate signals when the compound and the solvents were completely pure as traces of acetone or Cl^- accelerated the exchange. The $\Delta G^{\ddagger}$ of the exchange process, as calculated at the coalescence temperature, is 37 ± 2 kJ/mol (see the Experimental Section).

Scheme 1. Synthesis of the Ionic Complexes 11−13[a]

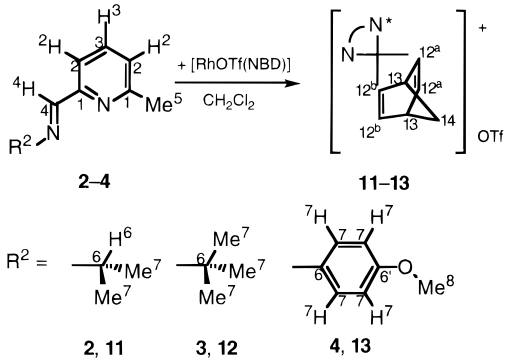

[a] For the sake of clarity the rhodium atom has been omitted.

It is important to note that on the imine hydrogen H(4) of complexes **11**−**13** a $^3J(^1H-^{103}Rh)$ coupling constant in the range of 2.1−2.6 Hz has been observed

Table 5. ^{13}C NMR of the Four-Coordinate Ionic Complexes 11−13

no.	C(1)	C(2)	C(3)	C(4)	C(5)	C(6)	C(7)	C(8)	C(12)	C(13)	C(14)
11[a,b]	164.7	131.8	142.8	169.1	23.7	56.6 (3)[c]	24.9		65.6	54.0	65.4
	157.1	127.7							(10)[c]	(3)[c]	(6)[c]
11[b,f,h]	163.8	131.2	142.2	167.8	22.8	64.5	24.5		*g*	53.3	*g*
	156.0	126.7									
12[b,d]	163.8	130.4	141.5	166.8	23.7	65.8	29.9		61.3	51.9[e]	64.5[e]
	155.4	127.2							(10)[c]		
12[b,f]	164.5	131.4	142.8	167.1	25.0	66.9[i]	30.6		65.8	53.1	*i*
	156.2	127.9									
13[a,b]	163.7	130.8	141.3	168.7	23.9	139.9 (2)[c]	115.1	56.0	63.5	52.2	63.7[e]
	155.0	128.6				155.0	123.1		(10)[c]	(3)[c]	

[a] ^{13}C NMR spectra were recorded at room temperature at 50.32 MHz. [b] CD_2Cl_2. [c] J(Rh−C) in Hz. [d] ^{13}C NMR spectra were recorded at room temperature at 75.47 MHz. [e] No coupling observed. [f] ^{13}C NMR spectra were recorded at 183 K at 75.47 MHz. [g] Has not been observed. [h] CF_3SO_3 has been observed at 127.6, 123.4, 119.1, and 114.9 ppm. [i] C(6) and C(14) probably overlap.

Table 6. ^{1}H NMR[a] of the Neutral Five-Coordinate Complexes 14−16

no. (T (K))	H(2)	H(3)	H(4)	H(5)	H(6) *H(8)*	H(7)	H(12)	H(13)	H(14)
14 (293)	7.47 [d, 1H]	7.75 [t, 1H]	8.34 [s, 1H]	3.61 [s, 3H]	4.33 [sp, 1H]	1.83 [d, 6H]	3.00 (2.3)[b] [br d, 4H][e]	3.57 [s,[c] 2H]	1.06 [s,[c] 2H]
	7.35 [d, 1H]								
14 (183)	7.42 [d, 1H]	7.74 [t, 1H]	8.32 [s, 1H]	3.35 [s, 3H]	4.05 [sp, 1H]	1.68 [d, 6H]	2.96 [s,[c] 4H][e]	3.50 [s,[c] 2H]	0.97 [s,[c] 2H]
	7.39 [d, 1H]								
15 (293)	7.48 [d, 1H]	7.72 [t, 1H]	8.37 [s, 1H]	3.74 [s, 3H]		1.88 [s, 9H]	2.92 (2.1)[b] [br d, 4H][e]	3.57 [s,[c] 2H]	1.03 [s,[c] 2H]
	7.35 [d, 1H]								
15 (183)	7.48 [d, 1H]	7.74 [t, 1H]	8.28 [s, 1H]	3.65 [s, 3H]		1.79 [s, 9H]	2.89 [s,[c] 2H][e]	3.49 [s,[c] 2H]	0.93 [s,[c] 2H]
	7.35 [d, 1H]						2.67 [s,[c] 2H][e]		
16 (293)	7.47[d] [d, 2H]	7.73 [t, 1H]	8.49 [s, 1H]	3.62 [s, 3H]	*3.92[e] [s, 3H]*	8.36 [d, 2H]	2.97 (2.1)[b] [br d, 4H][e]	3.41 [s,[c] 2H]	0.92 [s,[c] 2H]
16 (183)	7.43 [d, 1H]	7.58 [t, 1H]	8.53 [s, 1H]	3.48 [s, 3H]	*3.86[e] [s, 3H]*	8.32 [d, 2H]	2.87 [s,[c] 4H][e]	3.42 [s,[c] 2H]	0.93 [s,[c] 2H]
	7.38 [d, 1H]					7.01 [d, 2H]			

[a] ^{1}H NMR spectra were recorded in CD_2Cl_2 at 300.13 MHz; s = singlet, d = doublet, t = triplet, sp = septet, br = broad. [b] Residual coupling. [c] No coupling observed. [d] Accidental degenerate. [e] There is a clear temperature dependent chemical shift varying between 0.04 and 0.14 ppm.

(Table 4) at room temperature, for **12** the temperature range is 193−298 K, which shows that the nitrogen ligand remains coordinated on the NMR time scale. Also, at room temperature, a coupling constant of 2.1 Hz was observed on the olefinic hydrogen H(12) signals owing to coupling with ^{103}Rh (Table 4). The ^{103}Rh−^{13}C{^{1}H} coupling constants for C(12) and C(13) of **11**−**13**, for C(14) of the NBD ligand for complex **11**, and for C(6) in the case of complexes **11** and **13**, even at room temperature, corroborate the intramolecular nature of the exchange (Table 5).

Addition of N−N ligand **2** to complex **11** at 183 K caused extra line broadening of the H(12[a]) and H(12[b]) signals of which the rate $1/\tau$, measured on these signals, increased with increasing ligand concentration. However, no intermolecular ligand exchange occurred at 183 K, as the signals of the coordinated and noncoordinated nitrogen ligand remained sharp. When we increase the temperature, we also observe intermolecular exchange of the N−N ligand. Concentration-dependent measurements at 263 K showed that the rate $1/\tau$, measured on the Me-substituent of both complex **11** and the N−N ligand **2**, is linearly dependent on the concentration of the ligand and complex. The $1/\tau$ (Me) of the complex as a function of the ligand concentration goes through zero, implying that $1/\tau$ (complex) = k[**2**].

Synthesis and Characterization of [RhCl(2-(C(H)=N−R^2)-6-(Me)C$_5$H$_3$N)(NBD)]; R^2 = *i*-Pr (14), *t*-Bu (15), and *p*-Anisyl (16). Complexes **14**−**16** have been prepared in quantitative yield by reaction of the corresponding ligands **2**−**4** with [RhCl(NBD)]$_2$ in dichloromethane (Scheme 2). Ligand coordination was obvious from the chemical shift differences between the free and coordinated ligands for both the N−N and the NBD ligands (Tables 2, 3, 6, and 7).

The chemical shifts of the pyridine methyl hydrogen atoms H(5), the *i*-Pr hydrogen atoms H(6) and the *i*-Pr methyl atoms H(7), and the olefinic hydrogen atoms H(12), methine hydrogen atoms H(13), and the methylene hydrogen atoms H(14) of the NBD ligand of **14**−**16** are different from those of the ionic complexes **11**−**13**. From the relevant ^{1}H and ^{13}C NMR chemical shifts collected in Tables 8 and 9 it is clear from the alkene chemical shifts that complexes **14**−**16** have a trigonal bipyramidal (TBP) structure in solution.

Scheme 2. Reaction of the Nitrogen Ligands 2−4 with [RhCl(NBD)]$_2$ To Form 14−16[a]

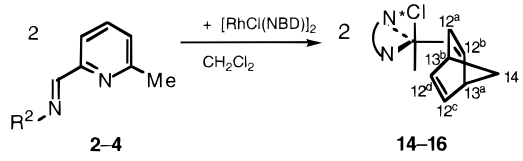

2–4 **14–16**

R^2 = *i*-Pr : **2** and **14**, *t*-Bu **3** and **15**, *p*-anisyl **4** and **16**

[a] For the sake of clarity the rhodium atom has been omitted.

Fluxional Processes. At 183 K, the olefinic hydrogen atoms H(12) of complex **15** appear as two signals and not as four, as one might expect, since the olefinic hydrogen atoms H(12[a]), H(12[b]), H(12[c]), and H(12[d]) (Scheme 2) should all be inequivalent for a five-coordinate TBP conformation if the geometry is analogous to the solid state structure of **14** (Figure 3). This is likely in view of the chemical shift values of the olefinic atoms (Tables 8 and 9). Also, the methine hydrogen atoms H(13[a]) and H(13[b]) appear as one signal, although two signals might be expected. The olefinic H(12) signals of complex **15** coalesced at 228 K with $\Delta G^{\ddagger} = -46 \pm 2$ kJ/mol. In the case of complexes **14** and **16**, the olefinic hydrogen atoms H(12) already appeared as one signal at 183 K, indicating very fast dynamic processes even below this temperature.

The observed coalescence pattern for **15** at 183 K shows fast exchange between the N and N* sites

Table 7. ^{13}C NMR of the Neutral Five-Coordinate Complexes 14−16

no.	C(1)	C(2)	C(3)	C(4)	C(5)	C(6)	C(7)	C(8)	C(12)	C(13)	C(14)
14[a,b]	161.0	126.7	137.5	159.7	27.6	62.6	25.1		35.3 (9)[c]	47.5[f]	58.1 (6)[c]
	153.0	124.5									
14[b,g]	162.1	127.8	138.3	160.6	27.7	62.3	25.5[h]		35.8[h]	47.7[f]	58.5[h]
	153.2	125.5									
15[b,e]	161.9	126.6	137.6	158.5	27.9	62.0	31.8		*i*	47.8[f]	58.0[h]
	153.4	124.9									
15[b,g]	162.0	127.5	138.5	159.3	28.7	62.7	32.2		35.1 (10)[c]	47.6[f]	57.8 (7)[c]
	153.3	125.7									
16[a,d]	159.8	126.3	136.8	156.4	27.1	131.3	124.2	55.3	35.9[f]	46.9[f]	57.5 (6)[c]
	152.5	124.7				142.6	114.1				

[a] ^{13}C NMR spectra were recorded at room temperature at 50.32 MHz. [b] CD_2Cl_2. [c] J(Rh−C). [d] $CDCl_3$. [e] ^{13}C NMR spectra were recorded at room temperature at 75.47 MHz. [f] No coupling observed. [g] ^{13}C NMR spectra were recorded at 183 K at 75.47 MHz. [h] Broad. [i] Has not been observed.

Table 8. Selected ^{1}H NMR Chemical Shifts (ppm) for the Olefinic H(12), Methine H(13), and Methylene H(14) Hydrogen Atoms for Different Geometries

	H(12)	H(13)	H(14)
Square Planar Complexes			
11−13	3.95−4.65[a]	3.85−4.07	1.18−1.45
[Rh(NBD)(monothio-β-ketonate)][b]	3.90−4.75	3.50−3.80	1.05−1.45
[Rh(NBD)(PPh_3)Cl][c]	4.17[d]	3.77	1.39
[Rh(NBD){(pyrazolyl)$_2$PhCH}]PF_6[e]	4.04[d]	3.60	1.13
Square Pyramidal Complexes			
[Rh(NBD)(dppp)($SnCl_3$)][f] 298 K	3.80	3.40	1.40
[Rh(NBD)(dppp)($SnCl_3$)][f] 243 K	3.81[d]	3.47	1.40
[Rh(NBD)(dppb)($SnCl_3$)][f] 298 K	3.69[d]	3.26	1.26
[Rh(NBD)(dppb)($SnCl_3$)][f] 243 K	3.73[d]	3.23	1.26
Trigonal Bipyramidal Complexes			
14−16	2.47−3.07[a]	3.42−3.57	0.93−1.06
17−19	2.65−3.03	3.35−3.56	0.91−1.05
[Rh(NBD)(PMe_2Ph)$_2$(Me)][g] 300 K	2.58[d]	3.14	0.91
[Rh(NBD)($PMePh_2$)$_2$(Me)][g] 253 K	2.76[d]	2.92[d]	0.82
[Rh(NBD)(PPh_3)(Me)][g] 238 K	3.20[d]	2.78[d]	0.93
[Rh(NBD)(bis(indazol-1-yl)pyridin-2′-ylmethane)]PF_6[h]	3.54[i]	3.96[i]	1.45[i]

[a] A range is given. [b] Reference 29. [c] Reference 26. [d] Average value. [e] Reference 35. [f] Reference 36. [g] Reference 37. [h] Reference 21. [i] $CDCl_3$.

Table 9. ^{13}C NMR Chemical Shifts (ppm) for the C(12), C(13), and C(14) Carbon Atoms for Different Geometries

	vinyl C(12)	methine C(13)	methylene C(14)
Square Planar Complexes[a]			
11−13	61.3−65.6[b] (10)[c]	51.9−54.0 (3)[d]	63.7−65.4 (6)[d]
[Rh(NBD)($Tp^{iPr,4Br}$)][e−g]	57.0,[h] 57.6 (9.7)[c]	50.8,[h] 50.6(2.0)[c]	62.7, 62.7 (6.1)[c]
[Rh(NBD){(pyrazolyl)$_2$PhCH}]PF_6[i]	59.8	50.2 (1.9)[c]	62.0 (6.2)[c]
Trigonal Bipyramidal Complexes			
14−16	35.1−35.9 (9−10)[b,d]	46.9−47.6[b,h]	57.5−58.1 (6−7)[b,c]
17−19	35.2−37.0 (9−10)[b,d]	46.9−47.9 (2−3)[b,d]	57.4−58.6 (6−7)[b,d]
[Rh(NBD)(Tp^{Me})][e,g]	41.9 (broad)	48.9 (2.5)[c]	59.5 (6.6)[c]
[Rh(NBD)(bis(indazol-1-yl)pyridin-2′-ylmethane)]PF_6[i,j]	41.4 (13)[c]	47.9 (2.7)[c]	59.0 (6.6)[c]

[a] Unfortunately, no ^{13}C NMR chemical shift could be found in the literature for square pyramidal NBD complexes of Rh(I). [b] A range is given. [c] Rh−C coupling. [d] Rh−C coupling is not in all cases observed. [e] Reference 20. [f] Two isomers, which differ in the positioning of one noncoordinating pyrazolyl group, were observed. [g] The nomenclature for tris(pyrazolyl)borate ligands and their complexes, as proposed by Trofimenko[38] is used. [h] No coupling observed. [i] Reference 35. [j] Reference 21.

rendering H(12^a) and H(12^b) (Scheme 2) equivalent as well as H(12^c) and H(12^d) and of course H(13^a) and H(13^b).

Addition of free ligand **2** (0.5 and 2.0 equiv) to a solution of complex **14** had no effect on the number and line widths of the ^{1}H NMR signals of the free ligand **2** and of complex **14** at 183−298 K. It is therefore clear that in the case of these five-coordinate complexes, no exchange occurs between free and coordinated ligand, in contrast to what we have observed for the ionic four-coordinate complex **11**. Although complexes **14**−**16** are nonconducting in dichloromethane (see the Experimental Section), the possibility of Cl^- exchange has to be taken into account for the higher temperature process. This has been strikingly demonstrated for a 1:1 mixture of the four-coordinate ionic complex **11** or **13** and the neutral five-coordinate complex **14** or **15**, as the resulting spectra at 183 K and at room temperature showed a weighted average of the spectra of **11** and **14** and of **12** and **15**, respectively, instead of the spectra of the separate species. It is clear that fast Cl^- exchange must occur either via dissociation of a small amount of Cl^- from the neutral complex or via an intermediate binuclear species with the Cl atom bridging between both Rh(I) atoms. Since chloride exchange will equilibrate all olefinic H(12) hydrogen atoms, it seems logical to assume that this is the main cause of the coalescence of the two olefinic H(12) signals to one in the temperature range from 228 K to room temperature in the case of complex **15**, where R^2 is the bulky *t*-Bu group. In the case of the less bulky substituents *i*-Pr (complex **14**) and *p*-anisyl (complex **16**), chloride exchange is clearly

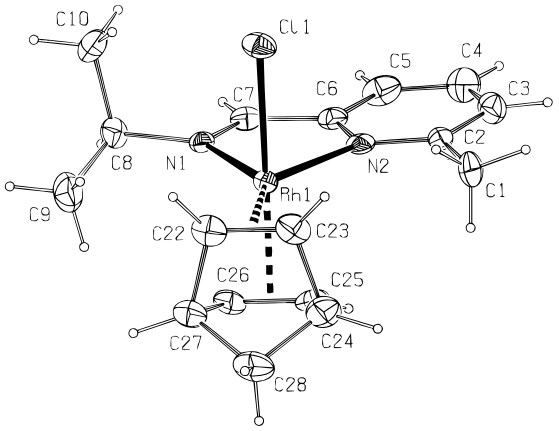

Figure 3. An ORTEP plot of complex **14** at 50% probability level along with the adopted numbering scheme.

Scheme 3. Synthesis of 17−19

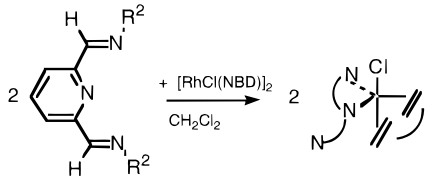

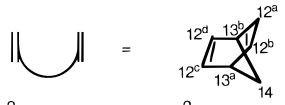

R^2 = *i*-Pr:**5** and **17**, R^2 = *t*-Bu: **6** and **18**, R^2 = *p* -anisyl: **7** and **19**.

easier, as at 183 K all four olefinic H(12) signals have already coalesced to one (Table 6).

Synthesis and Characterization of [RhCl(2,6-(C(H)=N−R^2)$_2$C$_5$H$_3$N)(NBD)]; R^2 = *i*-Pr (17), *t*-Bu (18), and *p*-Anisyl (19). The five-coordinate rhodium(I) complexes **17**−**19** have been prepared in virtually quantitative yield by adding the N−N−N ligands **5**−**7** to [RhCl(NBD)]$_2$ at room temperature in dichloromethane (Scheme 3). Coordination of the ligand and NBD was clear from chemical shift differences between the free and coordinated ligands (Tables 2, 3, 10, and 11). These complexes did not react further at room temperature, in contrast to the 1,5-cyclooctadiene complexes (*vide infra*). Corresponding complexes with the N−N−N ligands **8** and **9** could not be prepared.

Solid State Structures of 14 and 19. ORTEP plots at 50% probability level of **14** and **19**, along with their adopted numbering scheme, are given in Figures 3 and 4, respectively. Selected bond distances and angles have been collected in Table 12 for **14** and **19**.

The geometries of **14** and **19** around rhodium may be described as a distorted TBP, with the two nitrogen donor atoms of the nitrogen ligand and one alkene bond of norbornadiene in the equatorial plane. The chloride atom and the second alkene bond of norbornadiene are coordinated in the axial position. The N(1)−Rh(1)−N(2) angles of 73.53(16)° for complex **14** and of 72.91(9)° for complex **19** are both rather small when compared to other metal diimine complexes.[16−18] The rhodium atom of complexex **14** and **19** lies 0.058(1) and 0.068(1) Å, respectively, out of the N(1), N(2), C(22)═C(23) plane. The angle between the line connecting the rhodium atom with the center of the axial C(25)═C(26) bond and the line connecting the rhodium atom with the Cl(1) atom in the TBP is 16.0° in **14** and 13.9° in **19**.

In Table 13 reported bond lengths have been collected, for the sake of comparison, for square planar, square pyramidal, and trigonal bipyramidal rhodium norbornadiene complexes containing nitrogen ligands.

The Rh−Cl σ-bonds of **14** and **19**, which are 2.3972(17) and 2.3888(9) Å, respectively, are both shorter than those reported for five-coordinate square pyramidal (SP) rhodium chloride complexes.[16] This indicates, as expected for a TBP structure,[19] a stronger Rh−Cl σ-bond in the TBP geometry than in the SP geometry.

Also, it is clear that in complexes **14** and **19**, the π-back-bonding in the equatorial plane is stronger than that in the axial position, as indicated by the shorter Rh−C (olefinic) and longer C−C (olefinic) bonds for the equatorial alkene bond when compared to the longer Rh−C (olefinic) and shorter C−C (olefinic) bonds in the axial position. These features have also been observed for the TBP complexes [Rh(NBD)Tp^{Me})][20] and [Rh(NBD)(bis(indazol-1-yl)pyridin-2′-ylmethane))]PF$_6$ [21] (Table 13).

The Rh−N bond lengths in complexes **14** and **19** lie in the range from 2.248(4) to 2.283(3) Å and are comparable to the ones observed for rhodium(I) norbornadiene complexes with a TBP structure, but are 0.2 Å longer than those found for four-coordinate rhodium(I) norbornadiene compounds (Table 13). As in the case of the five-coordinate palladium and platinum complexes [(N−N)Pd(alkene)X$_2$] reported by Albano *et al.*,[22] the equatorial metal−nitrogen bonds in the TBP structures are longer than those in the corresponding four-coordinate square planar complexes, which may be ascribed to two factors.[22] Firstly, the electronic saturation of the metal atom in five-coordinate complexes weakens σ-donation. Secondly, there is less favorable overlap between the donor orbitals and the relevant metal orbitals due to the N−metal−N angle.[22]

Structure in Solution and Fluxional Behavior of 17−19. At 183 K, in CD_2Cl_2, the N−N−N ligands **5**−**7** in the complexes **17**−**19** are coordinated as bidentate ligands, as observed for **19** (see Figure 4), which is clear from the inequivalency of the meta pyridine hydrogen atom H(2), the imine hydrogen atoms H(4), and the H(6) and H(7) atoms of the *i*-Pr group. Also, the shifts of the methyl hydrogen atoms of the *t*-Bu group H(7) of complex **18** and the hydrogen atoms H(7) and H(8) of the *p*-anisyl ring of complex **19** (see Table 10) indicate bidentate bonding with a dangling imine side arm, in accord with the molecular structure (*vide supra*). ^{13}C NMR measurements for complex **17** at 183 K (Table 11) showed inequivalent imine side arms and two ^{13}C signals for C(12) and one ^{13}C signal for C(13), in agreement with the ^{1}H NMR spectra at 183 K (Table 10).

(16) Robertson, J. J.; Kadziola, A.; Krause, R. A.; Larsen, S. *Inorg. Chem.* **1989**, *28*, 2097.
(17) Iglesias, M.; del Pino, C. J. R.; Blanco, S. G.; Carrera, S. M. *J. Organomet. Chem.* **1988**, *338*, 89.
(18) Zassinovich, G.; Bettella, R.; Mestroni, G.; Bresciani-Pahor, N.; Geremia, S.; Randaccio, L. *J. Organomet. Chem.* **1989**, *370*, 187.
(19) Rossi, A. R.; Hoffmann, R. *Inorg. Chem.* **1975**, *14*, 365.
(20) Bucher, U. E.; Currao, A.; Nesper, R.; Rüegger, H.; Venanzi, L. M.; Younger, E. *Inorg. Chem.* **1995**, *34*, 66.
(21) López Gallego-Preciado, M. C.; Ballesteros, P.; Claramunt, R. M.; Cano, M.; Heras, J. V.; Pinilla, E.; Monge, A. *J. Organomet. Chem.* **1993**, *450*, 237.
(22) Albano, V. G.; Natile, G.; Panunzi, A. *Coord. Chem. Rev.* **1994**, *133*, 67.

Table 10. ^{1}H NMR[a] of the Five-Coordinate Complexes 17−19

no. (*T* (K))	H(2)	H(3)	H(4)	H(6) *H(8)*	H(7)	H(12)	H(13)	H(14)
17 (293)	7.90[b] [s, 3H]	7.90[b]	9.51 [s, 2H]	4.22 [sp, 2H]	1.65 [d, 12H]	2.99[c] [sd, 4H]	3.54 [s,[d] 2H]	1.06 [s,[d] 2H]
17 (183)	8.11 [d, 1H]	7.92 [t, 1H]	10.37 [s, 1H]	4.14 [br sp, 1H]	1.74 [br d, 6H]	3.00[c] [sd, 2H]	3.46 [s,[d] 2H]	0.96 [s,[d] 2H]
	7.60 [d, 1H]		8.40 [s, 1H]	3.96 [br sp, 1H]	1.30 [br d, 6H]	2.82[c] [sd, 2H]		
18 (293)	7.91[b] [m, 3H]	7.91[b]	9.57 [s, 2H]		1.72 [s, 18H]	2.94[c] [sd, 4H]	3.55 [s,[d] 2H]	1.04 [s,[d] 2H]
18 (183)	8.18 [d, 1H]	7.90 [t, 1H]	10.66 [s, 1H]		1.82 [s, 9H]	2.97[c] [sd, 2H]	3.47 [s,[d] 2H]	0.93 [s,[d] 2H]
	7.57 [d, 1H]		8.36 [s, 1H]		1.46 [s, 9H]	2.66[c] [sd, 2H]		
19 (293)	8.11 [d, 2H]	7.98 [t, 1H]	9.79 [s, 2H]	*3.91 [s, 6H]*	8.04 [br d, 4H]	3.03[c] [sd, 4H]	3.41 [s,[d] 2H]	1.02 [s,[d] 2H]
					7.10 [d, 4H]			
19 (183)	8.36 [d, 1H]	7.79 [t, 1H]	11.01 [s, 1H]	*3.88 [s, 3H]*	7.04 [d, 4H]	2.93[c] [sd, 4H]	3.35 [s,[d] 2H]	0.93 [s,[d] 2H]
	7.67 [d, 1H]		8.59 [s, 1H]	*3.84 [s, 3H]*	7.67 [d, 2H]			
					8.41 [d, 2H]			

[a] ^{1}H NMR spectra were recorded in CD_2Cl_2 at 300.13 MHz; s = singlet, d = doublet, t = triplet, sp = septet, br = broad. [b] H(2) and H(3) overlap. [c] There is a clear temperature dependent chemical shift between 0.08 and 0.13 ppm. [d] No coupling observed.

Table 11. ^{13}C NMR of the Five-Coordinate Complexes 17−19

no.	C(1)	C(2)	C(3)	C(4)	C(6)	C(7)	C(8)	C(12)	C(13)	C(14)
17[a,b]	154.6	125.8	137.9	160.2	62.6	24.8		36.6 (10)[c]	47.6 (3)[c]	58.1 (7)[c]
17[d,e]	154.0	125.4	137.3	159.5	62.1	24.4		35.4 (10)[c]	46.9 (2)[c]	57.7 (7)[c]
17[b,g]	155.6	128.8	139.1	161.9	63.8	26.5-		36.2[h] 35.2[h]	47.9[f]	58.6[f]
	153.2	124.6		159.8	63.6	24.5[h,i]				
18[d,e]	154.8	125.5	137.2	157.4	57.4	30.5		35.3 (10)[c]	47.2[f]	57.4 (6)[c]
18[b,g]	156.5	129.1	139.0	159.1	63.3	32.1		*j*	48.1[f]	56.0[f]
	153.7	124.3		158.2	60.2	30.2				
19[a,b]	154.8	126.4	138.1	158.0	160.4	124.5	114.9	37.0 (9)[c]	47.8[f]	58.5 (6)[c]
					143.5					

[a] ^{13}C NMR spectra were recorded at room temperature at 50.32 MHz. [b] CD_2Cl_2. [c] *J*(Rh−C). [d] ^{13}C NMR spectra were recorded at room temperature at 75.47 MHz. [e] $CDCl_3$. [f] No coupling visible. [g] ^{13}C NMR spectra were recorded at 183 K at 75.47 MHz. [h] Broad. [i] Range. [j] Was not observed.

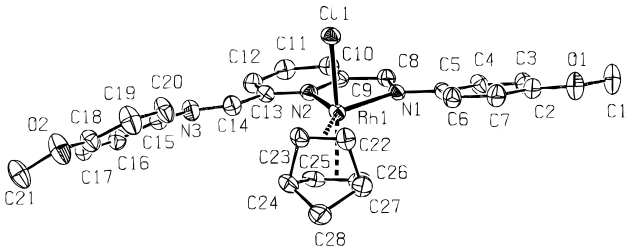

Figure 4. An ORTEP plot of complex **19** at 50% probability level along with the adopted numbering scheme. The hydrogen atoms and the cocrystallized molecule of dichloromethane have been left out for clarity.

At this temperature of 183 K, the spectral features of the diene ligand are similar to the ones observed for complexes **14**−**16**. In the case of complexes **17** and **18**, the olefinic hydrogen resonances H(12) have split into two signals instead of four, while only one signal appeared for the methine atoms H(13) instead of two. In the case of **19**, only one signal has been observed for the olefinic hydrogen atoms H(12) at 183 K. The fluxional processes that are responsible for this occurrence are clearly not due to intermolecular exchange of the N−N−N ligands, as addition of 0.5 equiv of free ligand to complex **18** had no effect at all on the ^{1}H NMR spectra in the range of 183−298 K.

In the temperature range of 183−218 K, the two olefinic H(12) hydrogen signals coalesced to one signal, while at the same time, the signals of the nonequivalent side arms coalesced for both complex **17** and **18**. At room temperature, the ^{13}C NMR spectra also show the magnetic equivalence of the imine side arms and one C(12) signal, in accord with the ^{1}H NMR data. Furthermore, we have found that the addition of chloride anions caused the dissociation of the nitrogen ligands. As the analogous triflate complexes could not be prepared, it was not possible to investigate the existence of chloride exchange in analogy to complexes **14** and **15**. Also, only chloride exchange would not explain the exchange of the coordinated and noncoordinated imine moieties. As a result, a more subtle mechanism has to occur (see the Discussion section).

Table 12. Selected Bond Distances and Angles of Complex 14 and 19

	14	**19**
Bond Distances (Å)		
Rh(1)−Cl(1)	2.3972(17)	2.3888(9)
Rh(1)−N(1)	2.248(4)	2.283(3)
Rh(1)−N(2)	2.255(5)	2.267(3)
Rh(1)−C(22)	2.063(6)	2.057(3)
Rh(1)−C(23)	2.063(6)	2.060(3)
Rh(1)− C(25)	2.123(5)	2.120(4)
Rh(1)−C(26)	2.127(6)	2.130(4)
C(22)−C(23)	1.429(8)	1.420(5)
C(25)−C(26)	1.404(8)	1.396(5)
Bond Angles (deg)		
Cl(1)−Rh(1)−N(1)	88.95(11)	89.41(7)
Cl(1)−Rh(1)−N(2)	89.34(12)	89.97(7)
Cl(1)−Rh(1)−C(22)	94.82(17)	95.02(13)
Cl(1)−Rh(1)−C(23)	93.87(18)	93.48(10)
Cl(1)−Rh(1)−C(25)	155.33(17)	154.79(11)
Cl(1)−Rh(1)−C(26)	158.26(17)	158.44(11)
N(1)−Rh(1)−N(2)	73.53(16)	72.91(9)
N(1)−Rh(1)−C(22)	123.47(19)	121.74(13)
N(1)−Rh(1)−C(23)	163.9(2)	162.04(12)
N(1)−Rh(1)−C(25)	113.8(2)	114.18(12)
N(1)−Rh(1)−C(26)	90.4(2)	89.98(12)
N(2)−Rh(1)−C(22)	162.5(2)	164.46(13)
N(2)−Rh(1)−C(23)	122.3(2)	124.76(12)
N(2)−Rh(1)−C(25)	88.20(19)	88.82(11)
N(2)−Rh(1)−C(26)	111.3(2)	110.41(12)

***In Situ* NMR Studies of the Reaction of [RhCl(COD)]$_2$ with the N−N−N Ligands 2,6-(C(R^1)=N−R^2)$_2$C$_5$H$_3$N (R^1 = H, R^2 = *i*-Pr (5), *t*-Bu (6), and *p*-Anisyl (7); R^1 = Me, R^2 = *i*-Pr (8), and *p*-Anisyl (9)).** Reactions between [RhCl(COD)]$_2$ and the nitrogen ligands **5**−**9** have been studied *in situ* because the intermediates of the reactions could not be isolated, owing to instability (Schemes 4 and 5).

When [RhCl(COD)]$_2$ was added to the N−N−N ligand **5** at 230 K in deuterodichloromethane, the COD complex

Table 13. Selected Crystallographic Data of Square Planar, Square Pyramidal, and Trigonal Bipyramidal Structures of Rhodium Norbornadiene Complexes Containing Nitrogen Ligands

	Rh−N (Å)	Rh−C olefinic (Å)	Rh−Cl (Å)	C−C olefinic (Å)
Square Planar Complexes				
[Rh(NBD){(pyrazolyl)$_2$PhCH}]PF$_6$[a]	2.08−2.10	2.07−2.09		1.33, 1.36
[Rh(NBD){(pyrazolyl)$_2$PhCH}][RhCl$_2$(NBD)][a,b]	2.078−2.089	2.101−2.125		1.384, 1.401
[Rh(NBD)(bpy)]Cl·H$_2$O[c]	2.064−2.074	2.125−2.139		1.390, 1.393
Square Pyramidal Complexes				
[Rh(NBD)(bpy)Cl][c]	2.094	2.098−2.123	2.590	1.424
[Rh(NBD)(2-(phenylazo)pyridine)Cl][c]	2.055−2.042	2.159−2.118	2.4958	1.401, 1.415
Trigonal Bipyramidal Complexes				
14	2.248−2.55 eq	2.063 eq	2.3972	1.429 eq
		2.123−2.127 ax		1.404 ax
19	2.267−2.283 eq	2.057−2.057 eq	2.3888	1.420 eq
		2.120−2.130 ax		1.396 ax
[Rh(NBD)(Tp^{Me})][d]	2.25[e] eq, 2.147 ax	1.95[f] eq, 2.05[f] eq		1.37 eq, 1.45 ax
[Rh(NBD)(bis(indazol-1-yl)pyridin-2′-ylmethane)]PF$_6$[g]	2.16−2.249 eq	2.09−2.14 eq		1.38 eq
	2.166 ax	2.11−2.21 ax		1.34 ax

[a] Reference 35. [b] Only data of the [Rh(NBD){(pyrazolyl)$_2$PhCH}] cation are given here. [c] Reference 16. [d] Reference 20. [e] Avarage. [f] The distance of Rh to the centers of the vinyl bonds are given here. [g] Reference 21.

Scheme 4. In Situ Formation of Complexes 20−22

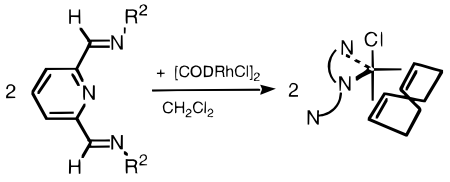

5–7 **20–22**

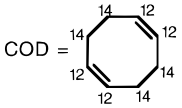

R^2 = *i*-Pr: **5** and **20**, R^2 = *t*-Bu: **6** and **21**, R^2 = *p*-anisyl: **7** and **22**.

Scheme 5. Reaction of [RhCl(COD)]$_2$ with Ligand 9 To Form 24

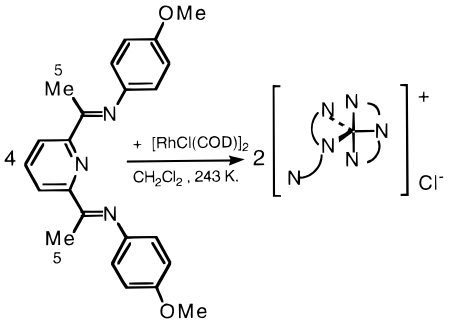

9 **24**

[RhCl(2,6-(C(H)═N−*i*-Pr)$_2$C$_5$H$_3$N)(COD)] (**20**) was initially formed, as may be concluded from the ^{1}H NMR spectra at 230 K (Table 14). The chemical shifts of the signals for the hydrogen atoms H(2), H(3), H(4), H(6), and H(7) are comparable to those found for complex **17** (Table 10). Raising the temperature to room temperature gave conversion of **20** to the deuterochloromethyl complex [RhCl$_2$(CD$_2$Cl)(2,6-(C(H)═N−*i*-Pr)$_2$C$_5$H$_3$N)] (**23**)[1] with concomitant formation of free COD.

When the reaction of [RhCl(COD)]$_2$ with the N−N−N ligand **6** was carried out in an NMR tube at 223 K, the complex [RhCl(2,6-(C(H)═N−*t*-Bu)$_2$C$_5$H$_3$N)(COD)] (**21**) was formed, which is probably a five-coordinate species, because the ^{1}H NMR spectrum of **21** (Table 14) at 213 K resembled the room temperature ^{1}H NMR spectrum of **18** (Table 10). It should be noted that in this case, with the bulky *t*-Bu group, the olefinic hydrogen atoms H(12) were observed as two signals at 223 K. Raising the temperature to the range of 233−273 K caused the equilibrium to move toward [RhCl(COD)]$_2$ and free ligand **6**.

Addition of the N−N−N ligand **7** to [RhCl(COD)]$_2$ at 230 K gave a fast reaction, as the mixture turned instantly from yellow to purple affording complex [RhCl(2,6-(C(H)═N−*p*-anisyl)$_2$C$_5$H$_3$N)(COD)] (**22**). At 243 K, the ^{1}H NMR spectrum of **22** (Table 14) is analogous to the room temperature spectrum of **19** (Table 10), indicating a similar structure. After 24 h at room temperature, no oxidative addition of dichloromethane had taken place, but instead, decomposition of **22** was observed.

[RhCl(COD)]$_2$ did not react with the N−N−N ligand **8**, but did react with ligand **9** in two steps. It should be noted that when in the temperature range of 190−240 K, 2 equiv of ligand **9** was used for 1 equiv of [RhCl(COD)]$_2$ and the dark green complex [Rh(2,6-(C(Me)═N−*p*-anisyl)$_2$C$_5$H$_3$N)$_2$]Cl (**24**) was initially formed (Scheme 5, Table 15) with unreacted [RhCl(COD)]$_2$ remaining in solution.

At 240 K, fluxional processes occurred for **24**, *e.g.*, as for H(7), a broad signal was observed. However, at 183 K, in the slow-exchange limit, one N−N−N ligand **9** coordinates as a terdentate ligand, as may be concluded from the ^{1}H NMR spectrum of H(2), which appeared as a doublet, and of H(5), which appeared as a singlet. The second N−N−N ligand **9** coordinates as a bidentate ligand, as H(2) appeared as two separated doublets, which is in accord with the observation that H(5) also occurs as two well-separated signals (Table 15).

Increasing the temperature of the reaction mixture to 273 K caused the dark green complex **24** to react with excess [RhCl(COD)]$_2$ to form the green square planar rhodium complex [RhCl(2,6-(C(Me)═N−*p*-anisyl)$_2$C$_5$H$_3$N)] **25** (Scheme 6), which was not isolated from the mixture but identified by comparison with an authentic sample.[1] ^{13}C NMR measurements could not be carried out because of the instability of the relevant intermediates.

A further temperature increase to 298 K gave, as expected, oxidative addition of dichloromethane yielding the orange chloromethyl complex [RhCl$_2$(CD$_2$Cl)(2,6-(C(Me)═N−*p*-anisyl)$_2$C$_5$H$_3$N)] (**26**), of which the isolation and characterization have been described elsewhere.[1] It should be noted that Rh(III) complexes

Table 14. ^{1}H NMR[a] of the Five-Coordinate Complexes 20−22

no.	*T* (K)	H(2)	H(3)	H(4)	H(6) *H(8)*	H(7)	H(12)	H(14)
20	230	7.96 [m, 3H][b]	*b*	9.4 [br s, 2H]	4.27 [br m, 2H]	1.53 [d, 12 H]	2.99 [s,[c] 4H]	2.36 [s,[c] 4H] 1.6 [m, 4H]
21	223	7.96 [m, 3H][b]	*b*	9.6 [br s, 2H]		1.56 [s, 18H]	3.87 [s,[c] 2H] 3.22 [s,[c] 2H]	2.47 [s,[c] 2H] 2.21 [s,[c] 2H] 1.56 [s,[c] 4H]
22	243	8.05 [d, 2H]	7.87 [t, 1H]	9.73 [s, 2H]	*3.90 [s, 6H]*	7.95 [br d, 4H] 7.04 [d, 4H]	3.62 [s,[c] 4H]	2.09 [s,[c] 4H] 1.42 [d, 4H]

[a] ^{1}H NMR spectra were recorded at 300.13 MHz; s = singlet, d = doublet, t = triplet, br = broad, m = multiplet. [b] H(2) and H(3) overlap. [c] No coupling observed.

Table 15. ^{1}H NMR of the Complex 24[a]

T (K)	H(2)	H(3)	H(5)	H(7)[c]	H(8)[c]
240	7.85 [d, 4H]	8.07[b] [d, 2H]	1.79 [s, 12H]	6.57 [d, 8H], 6.28 [br d, 8H]	3.74 [s, 12H]
183	*7.89 [d, 1H]*	*7.64*[b] *[t, 1H]*	*2.19 [s, 3H]*	6.57 [s, 6H], 6.51 [s, 2H], 6.42 [d, 2H]	3.70 [br d, 12H]
	7.81 [d, 1H]	8.15[b] [t, 1H]	*1.14 [s, 3H]*	6.39 [d, 2H], 6.21[d, 2H] 5.71 [d, 2H]	
	7.93 [d, 2H]		1.86 [s, 6H]		

[a] ^{1}H NMR spectra were recorded at 300.13 MHz; s = singlet, d = doublet, dd = double doublet, t = triplet, sp = septet, br = broad. The numbers in *italics* refer to the bidentate coordinated ligand. [b] There is a clear temperature dependent chemical shift. [c] Differentiation between hydrogen atoms belonging to the terdentate ligand and to the bidentate coordinated ligand is not possible.

Scheme 6. Reaction of 24 with $[RhCl(COD)]_2$ To Form 25 and Subsequently 26

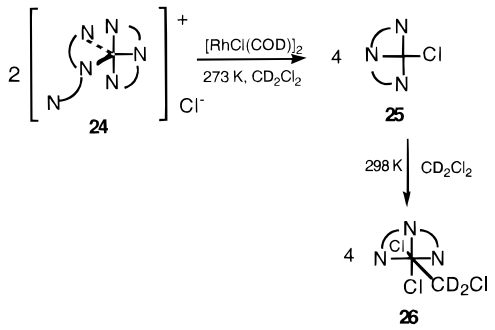

$[RhCl_2(CD_2Cl)(2,6\text{-}(C(R^1)=N-R^2)_2C_5H_3N)]$ (R^1 = H, R^2 = *i*-Pr, *t*-Bu, cyclohexyl, *p*-anisyl; R^1 = Me, R^2 = *p*-anisyl, *i*-Pr) have been prepared via $[RhCl(2,6\text{-}(C(R^1)=N-R^2)_2C_5H_3N)]$ from $[RhCl(alkene)_2]_2$ (alkene = ethene or cyclooctene) and the corresponding N−N−N nitrogen ligands in CH_2Cl_2.[1]

Discussion

Previously, we have reported the synthesis of the planar Rh(I) complexes $[RhCl(2,6\text{-}(C(R^1)=N-R^2)_2C_5H_3N)]$ (R^1 = H, R^2 = *i*-Pr, *t*-Bu, cyclohexyl, *p*-anisyl; R^1 = Me, R^2 = *p*-anisyl, *i*-Pr) by reacting $[RhCl(alkene)_2]_2$ (alkene = ethene, cyclooctene) with the corresponding N−N−N nitrogen ligands.[1] These apparently highly nucleophilic complexes rapidly underwent oxidative addition of substrates containing C−Cl bonds.[1] However, no reaction was observed with H_2 and alkenes, even under high pressure, or when the complex contained good leaving groups X^-. We considered this rather remarkable and focused our attention, therefore, on stabilizing rhodium−alkene bonds by a different route. Since reaction of $[RhCl(ethene)_2]_2$ with the N−N−N ligands easily led to substitution of ethene, we used more strongly bonding alkenes like COD and the more rigid NBD in the starting compound so that rupture of the $RhCl_2Rh$ bridge would dominate over alkene substitution. We indeed observed that reaction (Scheme 3) of $[RhCl(NBD)]_2$ with the N−N−N ligands **5**−**7** afforded **17**−**19**, which for **19** was shown to have a distorted TBP structure in the solid state (Figure 4). From the single-crystal X-ray studies on **14** (Figure 3) and **19** (Figure 4), it is clear that not only the N−N ligand in **14** but also the N−N−N ligand in **19** is bonded as a bidentate ligand with the pyridyl N-atom and one imine N-atom bonded to Rh(I) in the equatorial plane. The NBD ligand is bonded as a bidentate ligand with one alkene bond in the equatorial plane and the other alkene bond in an axial position; the other axial position is occupied by the chloride atom. The long Rh−N bonds and the small N−Rh−N bite angles are typical for these complexes, although both N-atoms are in the equatorial plane.[22] It is clear that this five-coordinate geometry is stabilized by steric bulk close to the coordinated N-atoms, as rationalized extensively for Pd complexes.[22,23]

Although fluxional movements (*vide infra*) occur in all five-coordinate complexes reported here, it is clear from the alkene chemical shifts at higher and lower temperatures that the TBP geometry is the ground state conformation also in solution (Table 8 and 9). It is interesting to note that these five-coordinate NBD complexes **17**−**19** did not react further, which allowed us to study their dynamic behavior (*vide infra*).

However, in the case of reactions of $[RhCl(COD)]_2$, it turned out that the intermediates and products that were observed depended strongly on the R^1 and R^2 substituents of the N−N−N ligands **5**−**9**, as discussed in the Results section.

In view of these and previous results,[1] we suggest the tentative general reaction scheme shown in Scheme 7. In step i, the chloride bridge is ruptured with formation of the five-coordinate NBD complexes **17**−**19** and COD complexes **20**−**22**. The reaction sequence now proceeds with step ii, which involves substitution, but only for COD, to give complex **24** with R^1 = Me and R^2 = *p*-anisyl which, in the presence of $[RhCl(COD)]_2$ at 273 K, afforded the planar **25** (step iii), and subsequently at 298 K converted to **26** (step iv).

Fluxional Processes. In order to look more closely into the origins of the dynamic behavior of complexes **17**−**19**, the new compounds **14**−**16** (Scheme 2) have been prepared, which turned out to have very similar variable temperature ^{1}H NMR spectra. In addition, the ionic complexes **10**−**13** (Scheme 1 and Figure 1) have been prepared, which contain asymmetric and symmetric bidentate N−N ligands. For the sake of simplic-

(23) Johnson, L. K.; Killian, C. M.; Brookhart, M. *J. Am. Chem. Soc.* **1995**, *117*, 6414.

Scheme 7. Reaction of Nitrogen Ligands Containing Three N-Donor Atoms with [RhCl(diene)]$_2$ in CD_2Cl_2 To Give Chloromethyl Complexes

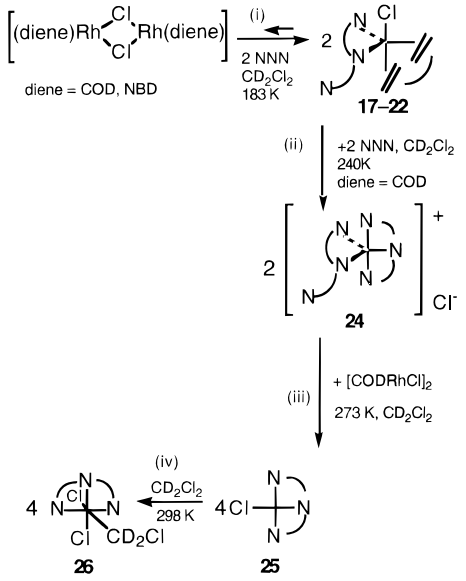

ity, we commence our discussion with the ionic complexes. The unusually dark colored compound **10** is unfortunately rather insoluble, but it was possible to observe for the bpm ligand that the H(2) and H(2′) hydrogen atom signals, which are inequivalent at 183 K, merge and become magnetically equivalent at 293 K (Figure 2). This process may be due, if it is intramolecular, to the mechanism proposed by Pregosin *et al.*[24] and Bäckvall and Gogoll,[25] which involves intermediates with monodentate bpm ligands as shown in Scheme 8. We have also found that an intermolecular exchange of bpm occurred when free bpm was added, but owing to the low solubility, the kinetics of the reaction could not be investigated.

Therefore, it was interesting to study the square planar complex **11** with and without extra N−N ligand **2**. At 183 K, the H(12^a) and H(12^b) signals of the NBD ligand, which are already broadened, are observed separately at 4.08 and 4.64 ppm (Table 4), while at 195 K, they have coalesced to one signal at 4.45 ppm. As ^{103}Rh−H coupling is observed for the H-atom on the imine C-atom between 195 and 293 K and on the H(12) of NBD, an intramolecular process occurs in the absence of free ligand. However, addition of free ligand at 183 K causes extra broadening of the H(12^a) and H(12^b) signals; this process has been shown to be ligand dependent, but without intermolecular ligand exchange, as the ligand and free ligand signals remain sharp. Therefore, it appears likely that the added N−N ligand **2** coordinates temporarily to the rhodium complex. The resulting five-coordinate intermediate exchange of H(12^a) and H(12^b) may now occur via Berry-type pseudorotational processes. In this respect, it is interesting that slight amounts of Cl^- or acetone may also enhance the alkene site-exchange rates of complex **2**, probably via five-coordinate intermediates.[26−30] However, intermediates with monodentate ligands are also possible in the light of mounting evidence for N−N ligands.[24,25,31]

Scheme 8. Mechanism for Exchange of the Four N-Atoms in 10

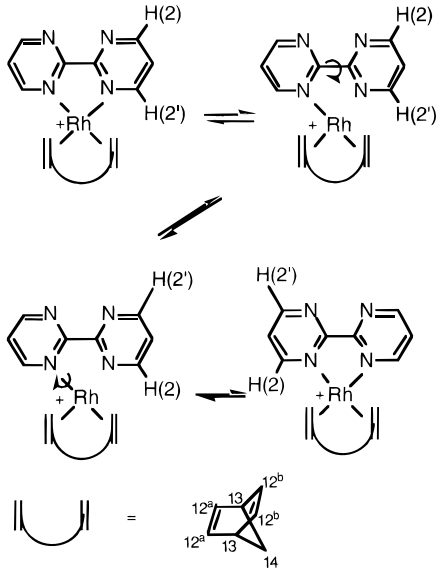

When we increase the temperature, intermolecular ligand exchange becomes feasible, but at lower rates than the previous process. The intermolecular ligand exchange could be measured quite precisely by studying the inverse of the lifetime ($1/\tau$) at 263 K on the signals of the methyl substituent of the coordinated and noncoordinated nitrogen ligand **2** as a function of the concentrations of both ligand **2** and complex **11**. The $1/\tau$ (complex) versus ligand concentration line goes through the zero point of this $1/\tau$ axis, indicating the virtual absence of a ligand independent pathway for intermolecular ligand exchange (see the Results section). At high ligand concentrations, a small signal of the imine proton appears at 9.93 ppm. This species might be [Rh(NBD)(2-(C(H)=N−*i*-Pr)-6-(Me)C_5H_3N)$_2$]-OTF with two monodentate bonded N−N ligands **2**, which are coordinated via the pyridine N-atoms. The high-chemical shift value may be rationalized when the imine protons of the two ligands are situated below and above the coordination plane.[31,32]

The five-coordinate complexes **15**, which contains N−N ligand **3**, and **17** and **18**, which contain the N−N−N ligands **5** and **6**, respectively, show only two vinyl H(12) signals instead of four and one methine H(13) signal instead of two (Tables 6 and 10) in the ^{1}H NMR spectra at 183 K. In all other cases (complexes **14**, **16**, and **19**), only one H(12) signal has been observed at 183 K indicating that we are dealing with very low energy pathways. Although no ^{103}Rh−H coupling constant could be found on the imine hydrogen atom for any of these five-coordinate complexes, we can exclude intermolecular ligand exchange in the temperature range from 183 to 298 K, as the free ligand signals remain sharp for mixtures of the complex and the free

(24) Albinati, A.; Kunz, R. W.; Ammann, C. J.; Pregosin, P. S. *Organometallics* **1991**, *10*, 1800.
(25) Gogoll, A.; Örnebro, J.; Grennberg, H.; Bäckvall, J.-E. *J. Am. Chem. Soc.* **1994**, *116*, 3631.
(26) Vrieze, K.; Volger, H. C.; Praat, A. P. *J. Organomet. Chem.* **1968**, *14*, 185.
(27) Vrieze, K.; Volger, H. C.; Leeuwen, P. W. N. M. *Inorg. Chim. Acta Rev.* **1969**, *3*, 109.
(28) Vrieze, K.; van Leeuwen, P. W. N. M. *Prog. Inorg. Chem.* **1971**, *14*, 1.
(29) Heitner, H. I.; Lippard, S. J. *J. Am. Chem. Soc.* **1970**, *92*, 3486.
(30) Heitner, H. I.; Lippard, S. J. *Inorg. Chem.* **1972**, *11*, 1447.
(31) Crociani, B.; Di Bianca, F.; Paci, M.; Boschi, T. *Inorg. Chim. Acta* **1988**, *145*, 253.
(32) van der Poel, H.; van Koten, G.; Vrieze, K. *Inorg. Chim. Acta* **1981**, *51*, 253.

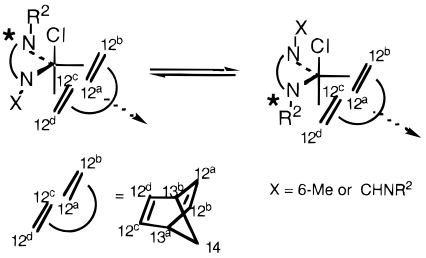

Figure 5. Exchange of N and N* sites in complexes **15**, **17**, and **18**.

ligands (see the Experimental Section). Also, this low-temperature process cannot be explained by Cl^- exchange processes, as models show that the dissociation of Cl^- and the subsequent reassociation of the anion to the ionic planar four-coordinate intermediates would always lead to the equilibration of the four vinyl H(12) protons, which is definitely not occurring for **15**, **17**, and **18** at 183 K. Although complex **14** with $R^2 = i$-Pr could not be used for the study of the behavior of this group, the four expected H(12) signals have already coalesced to one signal at 183 K; we were fortunate to have complex **17** with $R^2 = i$-Pr. It is very interesting to observe that at 183 K, the N−N−N ligand of **17** is bonded as a bidentate ligand (Scheme 3) with inequivalent *i*-Pr groups. However, and this is important, the two methyl groups on each *i*-Pr group are *enantiotopic* on the NMR time scale, while four *diastereotopic* methyl groups would have been expected for the TBP geometry, which is clearly the ground state conformation in solution (Scheme 3, Tables 8 and 10).

At this stage it is useful to consider some topological points before the possible physical movements of the ligands are explained. We may imagine, firstly, a mirror plane through the Rh−Cl axis and the midpoints of the coordinated alkene bonds that is caused by the interchange of the N and N* sites on the NMR time scale at 183 K (Figure 5). This site exchange would equilibrate H(12^a) with H(12^b), H(12^c) with H(12^d), and also the methine protons H(13^a) and H(13^b). When we now consider the possible physical movements, we should note that a simple turnstile rotation would give two H(12) signals and one methine H(13) signal as H(12^a) interchanges with H(12^c), H(12^b) with H(12^d), and further H(13^a) with H(13^b). However, this would not lead to the equilibration of diastereotopic Me groups on each *i*-Pr substituent to enantiotopic Me groups, and therefore, a turnstile rotation is not occurring.

It is very interesting to note that in the case of [Rh(Me)(NBD)(PMe_2Ph)$_2$], which also has a TBP structure with the two phosphine ligands in the equatorial plane, an axial−equatorial exchange of the alkene bonds occurred via Berry pseudorotational movements or via a turnstile mechanism.[33] However, over the whole temperature range studied, site exchange of the two equivalent phosphines definitely did not occur, as the two methyl groups on each P-atom remained diastereotopic. This is, therefore, in contrast to our case where the methyl groups on each inequivalent *i*-Pr group became enantiotopic.

As for complex **17**, neither a turnstile mechanism around the arrow in Figure 5 nor the Berry pseudorotational movement proposed by Shapley and Osborn is possible,[33] so we suggest that the variable temperature NMR data can be rationalized by a process involving a monodentate coordinated nitrogen ligand. This would lead, in principle, to two planar intermediates A and B for **17** and **18** (Figure 6).

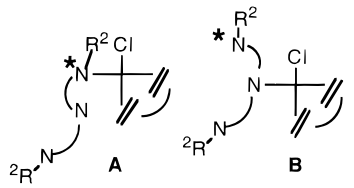

Figure 6. A possible exchange of N and imine N* sites in complexes **17** and **18** via an intermediate with a monodentate bonded ligand.

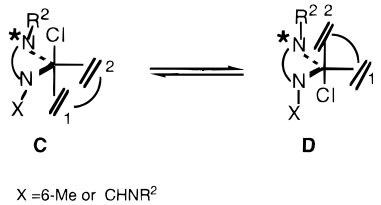

Figure 7. Permutation of Cl and both alkene bonds in **15**, **17**, and **18**.

In the case of A, where the *imine* N*-atom remains bonded to the Rh-atom, rotation of 180° about the Rh−N* bond and association of the pyridyl N-atom to Rh would indeed lead to N−N* exchange. Intermediate **B** is not possible for **17** and **18** since, when the *pyridyl* N-atom is only bonded to Rh, there would be two dangling imine side arms which, as they have equal chance to become bonded to Rh, would equilibrate both side arms, which is definitely not observed for **17** and **18** at 183 K.

So, with the mirror plane through the Rh−Cl axis and the midpoints of the coordinated alkene bonds, site exchange of N and N* can only occur via a monodentate bonded N−N* ligand via intermediate **A** in which only the imine N is bonded (Figure 6).

As a second topological alternative, we may visualize, on the NMR time scale, a mirror plane in the equatorial plane (Figure 7). We must then have an exchange between species **C** and **D**, which explains that the two methyl groups on each *i*-Pr group are enantiotopic while the two *i*-Pr groups remain inequivalent. It is obvious that we do not need to assume an intermediate monodentate nitrogen ligand, although this is not excluded. However, the axial chloride atom must move to the opposite axial position. A turnstile mechanism is again not possible. A possible pathway has been described by Shapley and Osborn,[33] Scheme D in their publication, which involves a permutation of the Cl-atom and both alkene bonds via a movement of the Cl-atom from one face to another of the pseudotetrahedral conformation of the other ligands. In this way, the coalescence from four to two signals may be rationalized and at the same time the interchange of N and N* sites. This last mechanism appears, however, to be a rather difficult one, and therefore, we prefer the mechanism shown in Figure 6 with **A** as the intermediate, which just involves exchange of N and N* via a monodentate intermediate. In light of the present knowledge[24,25,34] and in view of our results, this is a very reasonable mechanism.

(33) Shapley, J. R.; Osborn, J. A. *Acc. Chem. Res.* **1973**, *6*, 305.

(34) Groen, J. H.; Elsevier, C. J.; Vrieze, K.; Smeets, W. J. J.; Spek, A. L. *Organometallics* **1996**, *15*, 3445.

(35) Ballesteros, P.; López, C.; López, C.; Claramunt, R. M.; Jiménez, J. A.; Cano, M.; Heras, J. V.; Pinilla, E.; Monge, A. *Organometallics* **1994**, *13*, 289.

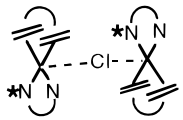

Figure 8. Proposed chloride exchange via a binuclear chloride species.

At higher temperatures, there is also a second dynamic process occurring in these five-coordinate complexes **15**, **17**, and **18**. In the case of complex **15** (Scheme 2), the two olefinic H(12) hydrogen atom signals observed at 183 K coalesced to one signal at 228 K with a $\Delta G^{\ddagger}$ of 46 kJ/mol, while for **14** with $R^2 = i$-Pr and **16** with $R^2 = p$-anisyl, the olefinic hydrogen atoms H(12) appeared at 183 K as one signal already. We have found that this equilibration is clearly due to chloride exchange. This has been nicely corroborated by the observation that a 1:1 mixture of ionic and five-coordinate complexes gave an ^{1}H NMR spectrum at 183 K with signals appearing at the weighted mean of those of the two complexes for both $R^2 = t$-Bu (**12** and **15**) and $R^2 = i$-Pr (**11** and **14**) with one signal for the H(12) protons. This chloride exchange probably proceeds via a binuclear chloride species (Figure 8). The process is faster for this 1:1 mixture of neutral **15** and ionic complex **12** than for the neutral five-coordinate complex **15** only. This is obvious as the concentration of the neutral chloride-donating complex is much higher for the 1:1 mixture than the concentration of dissociated Cl^- when only neutral complex is present, as also corroborated by the nonconductivity of complexes **14**−**16** (see the Experimental Section).

In order to form the binuclear intermediate shown in Figure 8, it appears logical to assume that the TBP conformation of complex **15** converts to square pyramidal conformation with the chloride atom on the axial position. This can be done by taking one of the bonded N-atoms as a pivot. After one pseudorotation, not only the diene spans an equatorial and an axial site but also the N−N* ligand. This will be a low-energy process as the ideal angle in this conformation is 90° instead of the 120° angle in the equatorial plane. If we now take the chloride anion, which is now on an equatorial position as a pivot, a square pyramidal intermediate conformation will result with the chloride on the axial position, as is needed for the formation of the binuclear intermediate (Figure 8).

In the case of the analogous complexes **17** and **18**, the two H(12) proton signals merge to one signal in the range from 183 to 218 K. However, a crucial observation is also that the signals of the inequivalent protons on the bidentate bonded N−N−N ligand coalesced, and

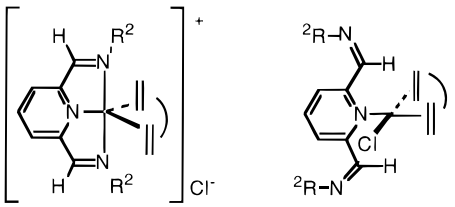

Figure 9. Intermediates in which the imine side arms take up equivalent positions.

with apparently the same $\Delta G^{\ddagger}$ of 40 ± 2 kJ/mol, showing that the bonded and nonbonded imine side arms interchange their sites. We have attempted to prepare ionic triflate complexes but without any success; therefore, we cannot provide evidence for chloride exchange. It was not possible to study chloride exchange by adding excess Cl^- as the added Cl^- replaced the N−N−N ligand on the complexes. Even if we had evidence for chloride exchange, *e.g.*, via a binuclear intermediate of the type shown in Figure 9, this would not explain the imine N site exchange for **17** and **18**, while it would only explain the coalescence of the two olefinic H(12) signals to one. Whatever the mechanism, it must involve intermediates in which the imine side arms preferably take up equivalent positions, as shown for the intermediates **E** and **F** in Figure 9 where **F** is in fact the same as **B** in Figure 6. The ionic five-coordinate intermediate **E** with a terdentate bonded N−N−N ligand and a dissociated chloride atom and the neutral four-coordinate intermediate **F** with a monodentate bonded N−N−N ligand, perpendicular to the coordination plane, and two dangling side arms fulfill this requirement. At the present time, we prefer intermediate **E**, as examples of dynamic exchange between bi- and terdentate bonded N−N−N ligands have been reported.[1] Also, for complex **24**, which contains both a bi- and a terdentate bonded N−N−N ligand, as demonstrated by ^{1}H NMR (Table 15) at 183 K, a dynamic exchange process occurs between both coordination modes which equilibrates both ligands at 240 K. Furthermore, intermediate **F** would lead to equilibration of the side arms but not to equilibration of the H(12) signals to one signal, but to two, if we do not exchange the alkene positions at the same time.

Acknowledgment. We would like to thank Professor P. W. N. M. van Leeuwen for stimulating discussions, Dr. H.-W. Frühauf for his interest in this work, and K. Goubitz for assistance with the crystallographic database.

Supporting Information Available: Further details of the structure determinations, including coordinates, bond lengths and angles, and thermal parameters for **14** and **19** (22 pages). Ordering information is given on any current masthead page.

OM960760B

(36) Garralda, M. A.; Pinilla, E.; Monge, M. A. *J. Organomet. Chem.* **1992**, *427*, 193.
(37) Rice, D. P.; Osborn, J. A. *J. Organomet. Chem.* **1971**, *30*, C84.
(38) Trofimenko, S. *Chem. Rev.* **1993**, *93*, 943.